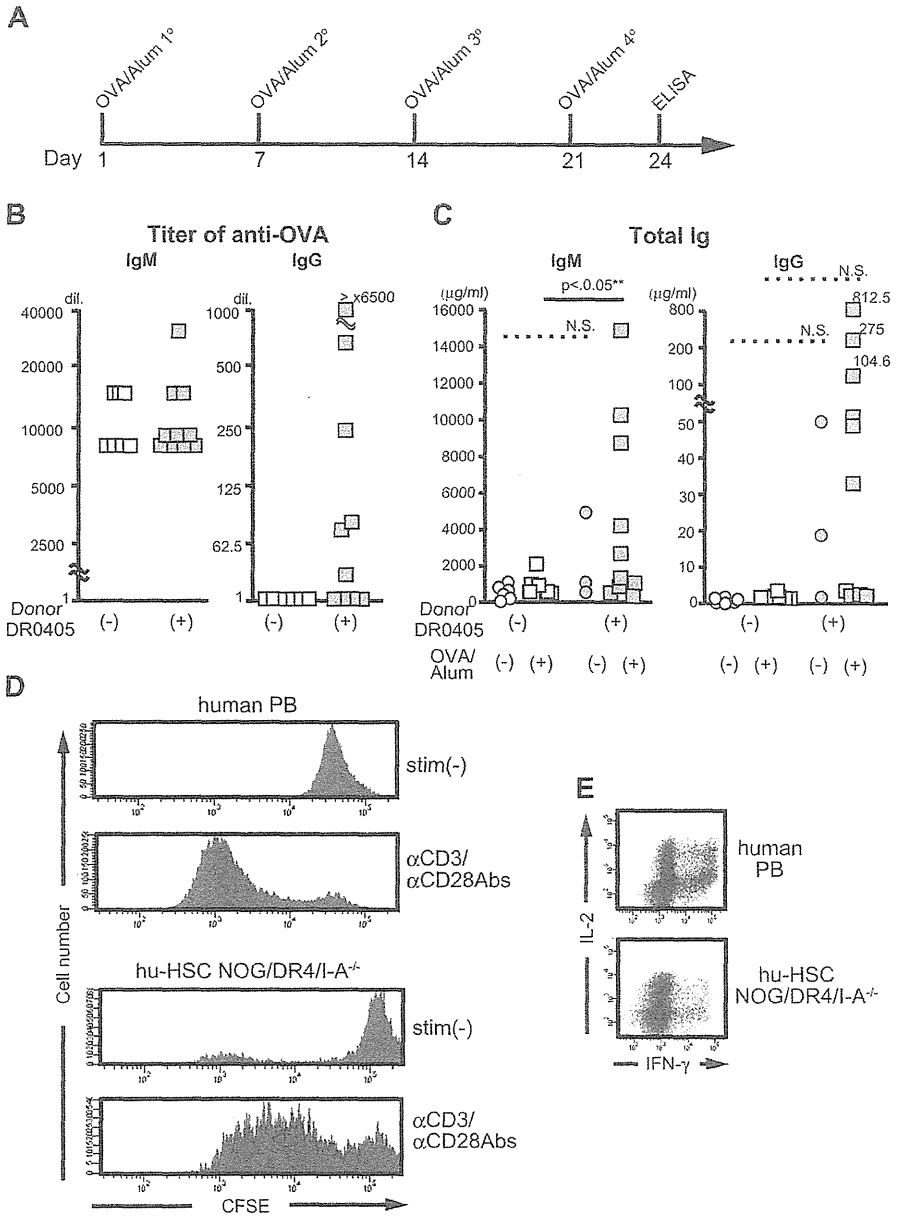

Fig. 4. Induction of humoral immune responses in hu-HSC NOG/DR4/I-A$^{-/-}$ mice. (A) Schematic protocol for OVA immunization. OVA (10 μg) and alum were injected intra-peritoneally into hu-HSC NOG/DR4/I-A$^{-/-}$ mice 20–25 weeks after HSC transplantation. After four weekly OVA immunizations, sera were collected and the presence of OVA-specific human IgM and IgG was examined by ELISA. (B) The production of anti-OVA antibody in the sera. The titers of OVA-specific IgM (left panel) and OVA-specific IgG (right panel) in sera from HLA-mismatched or HLA-matched HSC groups are shown. (C) The amount of total human IgM (left panel) and IgG (right panel) in sera. Sera were collected from HLA-mismatched (white symbols) or HLA-matched HSC groups (gray symbols) before (circles) and after (squares) the immunization with OVA and the Ig levels were quantified. (D) T-cell responses to stimulation with anti-CD3 and anti-CD28 antibodies. Splenocytes from hu-HSC NOG/DR4/I-A$^{-/-}$ mice with HLA-matched HSC were isolated 25 weeks after transplantation and compared with peripheral blood from a healthy human donor. Cells were labeled with CFSE and cultured *in vitro* in the presence of stimulating antibodies. At day 6, the cells were recovered and stained with anti-CD4. The dilution of CFSE was measured by flow cytometry. Representative flow plots are shown ($n > 10$). (E) Cytokine production by human CD4$^+$ T cells. *In vitro*-stimulated T cells from hu-HSC NOG/DR4/I-A$^{-/-}$ mice were re-stimulated with PMA/ionomycin in the presence of Golgi plug for 4 h at 37°C. The cells were fixed, permeabilized and stained with various anti-cytokine antibodies. Representative flow plots are shown ($n \geq 5$).

IgG in one mouse reached to >6250-fold higher than that of non-immunized control mice. OVA-specific IgG was not detected in hu-HSC NOG/HLA-DR4/I-Aβ$^{-/-}$ mice with HLA-mismatched HSC, although they showed OVA-specific IgM production (Fig. 4B). As for the total amount of IgM and IgG, there was no significant difference between the mice

with HLA-matched HSC and HLA-mismatched HSC before immunization (Fig. 4C, white symbols). After immunization, total IgM and IgG was increased in several mice in HLA-matched group, but none in HLA-mismatched group (Fig. 4C, gray symbols) and the increase was statistically significant for IgM, but not for IgG. These results suggested that humanized HLA transgenic mice with HLA-matched HSC transplantation mounted immune responses sufficient to induce antibody class switching in the human B cells.

We next analyzed T-cell function in the hu-DRB1:0405^{+} HSC NOG/HLA-DR4/I-A$\beta^{-/-}$ mice. The human T cells showed significant proliferation in response to anti-CD3 and anti-CD28 antibodies *in vitro*, and the activated T cells produced IL-2 and IFN-γ upon stimulation with PMA and ionomycin (Fig. 4D and E). These results suggested the presence of human T cells with normal function in the hu-HSC NOG/HLA-DR4/I-A$\beta^{-/-}$ mice. However, the magnitude of T-cell proliferation was not as robust as that of human T cells from normal healthy donors (Fig. 4D), and the amount of human IL-2 in the culture supernatants was not as high as that produced by normal human T cells (data not shown).

In the present study, using the novel mouse strain NOG/HLA-DR4/I-A$\beta^{-/-}$, we demonstrated that human lymphocytes that developed *in situ* in the humanized mice caused human humoral immune responses in an HLA-DR-restricted manner in cases that used HLA-matched HSC for transplantation. This is a significant advance in humanized mouse technology, as there has yet to be a reliable model in which properly functioning adaptive human immune responses occur without the need for xenotransplantation of human tissues (e.g. fetal liver and thymus in the BLT model) (23).

It has been speculated that the mismatch between the mMHC II responsible for the positive selection of human T cells in the mouse thymus and the HLA II expressed by human B cells in the periphery is the major obstacle to inducing functional human adaptive immune responses in conventional humanized mice (17). Our results demonstrated that this problem was overcome, even if partially, by the introduction of HLA II and the elimination of mMHC II. Recently, Danner *et al.* reported that antigen-specific human IgG was produced in NSG/HLA-DR mice that expressed a human/mouse chimeric molecule, in which the peptide-binding domain of the mouse I-Eβ chain was substituted with the corresponding domain of HLA-DRB1:0401 to mimic the structure of an HLA-DR4 molecule (24, 25). Because they used I-A sufficient NSG mice, the elimination of mMHC II was not necessary for the elicitation of human immune responses. However, it is noteworthy that the I-A sufficient NOG/HLA-DR4/I-A$\beta^{+/-}$ mice in our mouse colony did not induce human IgG responses (data not shown). One plausible explanation for these discrepant results is that mMHC II still played a dominant role in the positive selection of human T cells in I-A$^{+/-}$ mice because of the abundance of mMHC II^{+} TEC. This could render the size of the T-cell repertoire restricted by HLA II too small to induce detectable human immune responses. If this is the case, the elimination of mMHC II is critical to maximize the HLA-restricted T-cell repertoire.

Matching the HLA-DR haplotypes of the recipient NOG/DR4 transgenic mouse and donor HSC significantly influenced human T-cell homeostasis. In particular, HLA-matched reconstitution resulted in a large T_{EM} population, suggesting the HLA-dependent rapid proliferation of human T cells. Considering the extremely lymphopenic environment in NOG mice, the expansion of T_{EM} is reminiscent of lymphopenia-induced proliferation of T cells, which is a well-known phenomenon typically seen when a small number of T_{naive} are seeded into chronically lymphopenic environments (e.g. *RAG* gene deficiency or *scid* mutation) (20, 26). Thus, it is possible that a few human thymic immigrants proliferated to restore the T-cell compartment in NOG mice. This mechanism would explain the higher frequency and higher number of CD4^{+} T cells in the HLA-matched HSC group, compared with the mismatched group, at early time points. Although the same mechanism would also regulate the relatively slower increase of T cells in the HLA-mismatched group, in this case, mouse DC and Mϕ in NOG/DR4/I-A$^{-/-}$ mice predominantly stimulate the T cells, whereas both mouse and human APC would stimulate T cells in the HLA-matched HSC group. The difference in the abundance of APC is one reason for the difference in T-cell homeostasis between the HLA-matched and HLA-mismatched groups.

We previously demonstrated that human T cells in conventional hu-HSC NOG mice had extremely low proliferative capacity in response to antigenic stimulation (17). The accumulation of T_{EM} and the rapid decrease of T_{naive}, which have the largest capacity for proliferation, may be one possible explanation. Indeed, when the frequency of T_{naive} was increased by the transplantation of fetal thymic lobes from NOD mice into the renal capsules of NOG mice, human T cells showed strong proliferation in response to *in vitro* stimulation that was comparable to that of human T cells from healthy human adults (data not shown). This result suggests that high numbers of T_{naive} in NOG/DR4/I-A$^{-/-}$ mice will enable the augmentation of immune responses. There are two major mechanisms that regulate the size of the T_{naive} pool: the supply from the thymus (27, 28) and homeostatic proliferation in the periphery (29, 30). To enhance the function of the thymus (27), transgenic expression of keratinocyte growth factor or flt-3 ligand in TEC, which can enhance the regeneration of TEC after irradiation, should be tested (31,32,33,34,35). Regarding the homeostasis in the periphery, reconstitution of secondary lymphoid organs in NOG mice, which have a significant deficiency of lymph nodes (LN) (36,37,38), is important, as IL-7, a survival factor for T_{naive}, is provided by LN-resident reticular fibroblastic cells (39).

Humanized mice are an excellent tool with which to study human immunology. The reconstitution of a functional human adaptive immune system in hu-HSC NOG/HLA-DR4/I-A$\beta^{-/-}$ mice offers unique opportunities to test and utilize human immunity. For example, the capability to produce antigen-specific IgG in hu-HSC NOG/HLA-DR4/I-A$\beta^{-/-}$ suggests that this model has great potential for generating mAbs against various exogenous substances, such as viral or bacterial proteins. Such mAbs could work as therapeutic drugs for prevention of infection or allergy (18, 19). Along with further improvements of humanized mouse technologies, e.g. introduction of human cytokine genes (40,41,42), this mouse model will contribute to the development of new therapeutic strategies for human disease.

Supplementary data

Supplementary data are available at *International Immunology* Online.

Funding

Grant-in-Aid for Scientific Research on Priority Areas from the Ministry of Education, Culture, Sports, Science and Technology of Japan; a Grant-in-Aid for Scientific Research on Priority Areas awarded to K.S. (#19059001); a Grant-in-Aid for Scientific Research (S) from the Japan Society for the Promotion of Science awarded to M.I. (#18100005); a Grant-in-Aid for Scientific Research (C) from the Japan Society for the Promotion of Science awarded to T. T. (#23590561).

Acknowledgements

We thank M. Konno and E. Saijyo for their technical assistance.

Disclosure

The authors have no financial conflicts of interest.

References

1 Ito, M., Hiramatsu, H., Kobayashi, K. *et al.* 2002. NOD/SCID/gamma(c)(null) mouse: an excellent recipient mouse model for engraftment of human cells. *Blood* 100:3175.

2 Traggiai, E., Chicha, L., Mazzucchelli, L. *et al.* 2004. Development of a human adaptive immune system in cord blood cell-transplanted mice. *Science* 304:104.

3 Macchiarini, F., Manz, M. G., Palucka, A. K. and Shultz, L. D. 2005. Humanized mice: are we there yet? *J. Exp. Med.* 202:1307.

4 Ishikawa, F., Saito, Y., Yoshida, S., Harada, M. and Shultz, L. D. 2008. The differentiative and regenerative properties of human hematopoietic stem/progenitor cells in NOD-SCID/IL2rgamma (null) mice. *Curr. Top. Microbiol. Immunol.* 324:87.

5 Willinger, T., Rongvaux, A., Strowig, T., Manz, M. G. and Flavell, R. A. 2011. Improving human hemato-lymphoid-system mice by cytokine knock-in gene replacement. *Trends Immunol.* 32:321.

6 Ishikawa, F., Yoshida, S., Saito, Y. *et al.* 2007. Chemotherapy-resistant human AML stem cells home to and engraft within the bone-marrow endosteal region. *Nat. Biotechnol.* 25:1315.

7 Barabe, F., Kennedy, J. A., Hope, K. J. and Dick, J. E. 2007. Modeling the initiation and progression of human acute leukemia in mice. *Science* 316:600.

8 Dewan, M. Z., Terashima, K., Taruishi, M. *et al.* 2003. Rapid tumor formation of human T-cell leukemia virus type 1-infected cell lines in novel NOD-SCID/gammac(null) mice: suppression by an inhibitor against NF-kappaB. *J. Virol.* 77:5286.

9 Miyazato, P., Yasunaga, J., Taniguchi, Y., Koyanagi, Y., Mitsuya, H. and Matsuoka, M. 2006. *De novo* human T-cell leukemia virus type 1 infection of human lymphocytes in NOD-SCID, common gamma-chain knockout mice. *J. Virol.* 80:10683.

10 Baenziger, S., Tussiwand, R., Schlaepfer, E. *et al.* 2006. Disseminated and sustained HIV infection in CD34+ cord blood cell-transplanted Rag2-/-gamma c-/- mice. *Proc. Natl Acad. Sci. USA* 103:15951.

11 Sato, K., Misawa, N., Nie, C. *et al.* 2011. A novel animal model of Epstein-Barr virus-associated hemophagocytic lymphohistiocytosis in humanized mice. *Blood* 117:5663.

12 Kumar, P., Ban, H. S., Kim, S. S. *et al.* 2008. T cell-specific siRNA delivery suppresses HIV-1 infection in humanized mice. *Cell* 134:577.

13 Ito, A., Ishida, T., Utsunomiya, A. *et al.* 2009. Defucosylated anti-CCR4 monoclonal antibody exerts potent ADCC against primary ATLL cells mediated by autologous human immune cells in NOD/Shi-scid, IL-2R gamma(null) mice *in vivo*. *J. Immunol.* 183:4782.

14 Denton, P. W., Krisko, J. F., Powell, D. A. *et al.* 2010. Systemic administration of antiretrovirals prior to exposure prevents rectal and intravenous HIV-1 transmission in humanized BLT mice. *PLoS One* 5:e8829.

15 Ishikawa, F., Yasukawa, M., Lyons, B. *et al.* 2005. Development of functional human blood and immune systems in NOD/SCID/IL2 receptor {gamma} chain(null) mice. *Blood* 106:1565.

16 Hiramatsu, H., Nishikomori, R., Heike, T. *et al.* 2003. Complete reconstitution of human lymphocytes from cord blood CD34+ cells using the NOD/SCID/gammacnull mice model. *Blood* 102:873.

17 Watanabe, Y., Takahashi, T., Okajima, A. *et al.* 2009. The analysis of the functions of human B and T cells in humanized NOD/shi-scid/gammac(null) (NOG) mice (hu-HSC NOG mice). *Int. Immunol.* 21:843.

18 Kametani, Y., Shiina, M., Katano, I. *et al.* 2006. Development of human-human hybridoma from anti-Her-2 peptide-producing B cells in immunized NOG mouse. *Exp. Hematol.* 34:1240.

19 Becker, P. D., Legrand, N., van Geelen, C. M. *et al.* 2010. Generation of human antigen-specific monoclonal IgM antibodies using vaccinated "human immune system" mice. *PLoS One* 5:e13137.

20 Legrand, N., Cupedo, T., van Lent, A. U. *et al.* 2006. Transient accumulation of human mature thymocytes and regulatory T cells with CD28 superagonist in "human immune system" Rag2(-/-) gammac(-/-) mice. *Blood* 108:238.

21 Kouskoff, V., Fehling, H. J., Lemeur, M., Benoist, C. and Mathis, D. 1993. A vector driving the expression of foreign cDNAs in the MHC class II-positive cells of transgenic mice. *J. Immunol. Methods* 166:287.

22 Cosgrove, D., Gray, D., Dierich, A. *et al.* 1991. Mice lacking MHC class II molecules. *Cell* 66:1051.

23 Melkus, M. W., Estes, J. D., Padgett-Thomas, A. *et al.* 2006. Humanized mice mount specific adaptive and innate immune responses to EBV and TSST-1. *Nat. Med.* 12:1316.

24 Ito, K., Bian, H. J., Molina, M. *et al.* 1996. HLA-DR4-IE chimeric class II transgenic, murine class II-deficient mice are susceptible to experimental allergic encephalomyelitis. *J. Exp. Med.* 183:2635.

25 Danner, R., Chaudhari, S. N., Rosenberger, J. *et al.* 2011. Expression of HLA class II molecules in humanized NOD.Rag1-KO.IL2RgcKO mice is critical for development and function of human T and B cells. *PLoS One* 6:e19826.

26 Surh, C. D. and Sprent, J. 2008. Homeostasis of naive and memory T cells. *Immunity* 29:848.

27 Berzins, S. P., Uldrich, A. P., Sutherland, J. S. *et al.* 2002. Thymic regeneration: teaching an old immune system new tricks. *Trends Mol. Med.* 8:469.

28 Almeida, A. R., Rocha, B., Freitas, A. A. and Tanchot, C. 2005. Homeostasis of T cell numbers: from thymus production to peripheral compartmentalization and the indexation of regulatory T cells. *Semin. Immunol.* 17:239.

29 Jameson, S. C. 2002. Maintaining the norm: T-cell homeostasis. *Nat. Rev. Immunol.* 2:547.

30 Sprent, J. and Surh, C. D. 2011. Normal T cell homeostasis: the conversion of naive cells into memory-phenotype cells. *Nat. Immunol.* 12:478.

31 Min, D., Taylor, P. A., Panoskaltsis-Mortari, A. *et al.* 2002. Protection from thymic epithelial cell injury by keratinocyte growth factor: a new approach to improve thymic and peripheral T-cell reconstitution after bone marrow transplantation. *Blood* 99:4592.

32 Erickson, M., Morkowski, S., Lehar, S. *et al.* 2002. Regulation of thymic epithelium by keratinocyte growth factor. *Blood* 100:3269.

33 Kelly, R. M., Highfill, S. L., Panoskaltsis-Mortari, A. *et al.* 2008. Keratinocyte growth factor and androgen blockade work in concert to protect against conditioning regimen-induced thymic epithelial damage and enhance T-cell reconstitution after murine bone marrow transplantation. *Blood* 111:5734.

34 Kenins, L., Gill, J. W., Boyd, R. L., Hollander, G. A. and Wodnar-Filipowicz, A. 2008. Intrathymic expression of Flt3 ligand

enhances thymic recovery after irradiation. *J. Exp. Med.* 205:523.
35 Fry, T. J., Sinha, M., Milliron, M. *et al.* 2004. Flt3 ligand enhances thymic-dependent and thymic-independent immune reconstitution. *Blood* 104:2794.
36 Cao, X., Shores, E. W., Hu-Li, J. *et al.* 1995. Defective lymphoid development in mice lacking expression of the common cytokine receptor gamma chain. *Immunity* 2:223.
37 Park, S. Y., Saijo, K., Takahashi, T. *et al.* 1995. Developmental defects of lymphoid cells in Jak3 kinase-deficient mice. *Immunity* 3:771.
38 von Freeden-Jeffry, U., Vieira, P., Lucian, L. A., McNeil, T., Burdach, S. E. and Murray, R. 1995. Lymphopenia in interleukin (IL)-7 gene-deleted mice identifies IL-7 as a nonredundant cytokine. *J. Exp. Med.* 181:1519.
39 Link, A., Vogt, T. K., Favre, S. *et al.* 2007. Fibroblastic reticular cells in lymph nodes regulate the homeostasis of naive T cells. *Nat. Immunol.* 8:1255.
40 Willinger, T., Rongvaux, A., Takizawa, H. *et al.* 2011. Human IL-3/GM-CSF knock-in mice support human alveolar macrophage development and human immune responses in the lung. *Proc. Natl Acad. Sci. USA* 108:2390.
41 Rongvaux, A., Willinger, T., Takizawa, H. *et al.* 2011. Human thrombopoietin knockin mice efficiently support human hematopoiesis *in vivo*. *Proc. Natl Acad. Sci. USA* 108:2378.
42 Chen, Q., Khoury, M. and Chen, J. 2009. Expression of human cytokines dramatically improves reconstitution of specific human-blood lineage cells in humanized mice. *Proc. Natl Acad. Sci. USA* 106:21783.

Efficient Xenoengraftment in Severe Immunodeficient NOD/Shi-*scid* IL2rγ^{null} Mice Is Attributed to a Lack of CD11c$^+$B220$^+$CD122$^+$ Cells

Ryoji Ito,*,† Ikumi Katano,* Miyuki Ida-Tanaka,* Tsutomu Kamisako,* Kenji Kawai,* Hiroshi Suemizu,* Sadakazu Aiso,† and Mamoru Ito*

Xenograft animal models using immunodeficient mice have been widely applied in medical research on various human diseases. NOD/Shi-*scid*-IL2rγ^{null} (NOG) mice are known to show an extremely high engraftment rate of xenotransplants compared with conventional immunodeficient mice. This high engraftment rate of xenotransplants in NOG mice was substantially suppressed by the transfer of spleen cells from NOD-*scid* mice that were devoid of NK cells. These results indicate that cell types other than splenic NK cells present in NOD-*scid* mice but not in NOG mice may be involved in this suppression. To identify the cell types responsible for this effect, we transferred subpopulations of spleen cells from NOD-*scid* mice into NOG mice and assessed the levels of human cell engraftment after human PBMC (hPBMC) transplantation. These experiments revealed that CD11c$^+$B220$^+$ plasmacytoid dendritic cells (pDCs) from NOD-*scid* mice markedly inhibited engraftment of human cells. The CD11c$^+$B220$^+$ CD122$^+$ cells further fractionated from the pDCs based on the expression of CD122, which is an NK cell marker strongly inhibited during hPBMC engraftment in NOG mice. Moreover, the CD122$^+$ cells in the pDC fraction were morphologically distinguishable from conventional CD122$^+$ NK cells and showed a higher rejection efficiency. The current results suggest that CD11c$^+$B220$^+$ CD122$^+$ cells play an important role in xenograft rejection, and their absence in NOG mice may be critical in supporting the successful engraftment of xenotransplants. *The Journal of Immunology*, 2012, 189: 4313–4320.

We previously established the severely immunodeficient NOD/Shi-*scid*-IL2rγ^{null} (NOG) strain appropriate for generating a "humanized mouse" model in which human tissues, human cancers, and human PBMCs (hPBMCs) or cord blood hematopoietic stem cells (HSCs) can be engrafted or differentiated into multilineage immune cells after transplantation. Thus, these mice are useful as models for human tissue grafting (1, 2), cancer (3, 4), graft-versus-host disease (5), and the human immune system (6, 7). The success of xenoengraftment in NOG mice has been attributed to the multiple immunologic dysfunctions of acquired and innate immunity, whereby the lack of T and B cells and of NK cells is linked to the *scid* mutation (8) and to the IL-2 receptor common γ-chain deficiency (9), respectively.

The NOD strain in combination with the *scid* mutation or RAG deficiency is known to promote xenoengraftment. The recently reported signal regulatory protein-α (SIRP-α), which is a critical immune inhibitory receptor on macrophages, interacts with the CD47 ligand on the xenograft to prevent phagocytosis (10–12). Takenaka et al. (13) reported that the SIRP-α polymorphism on the NOD genetic background leads to enhanced binding to human CD47 and that this interaction may activate CD47-induced signaling pathways to support xenoengraftment. Furthermore, Shultz et al. (14) reported that complement-dependent hemolytic activity is more severely impaired in the NOD strain than in other inbred strains. These reports indicated that the NOD strain is much better than other strains in engrafting human cells and tissues. However, NOG mice showed a remarkably higher xenoengraftment level compared with NOD-*scid* mice despite having the NOD background. This higher xenoengraftment rate in NOG mice has been generally accepted as attributable to lack of NK cells as NOG mice lack NK cells through the introduction of an *IL-2Rγ* mutation. In fact, several reports have described how NK cells are important for xenograft rejection in immunodeficient mice. Higher success rates for xenoengraftment after transplantation of human HSCs were observed in NOD-*scid* β2m^{null} mice, which lack NK activity, and in NOD-*scid* mice treated with CD122 Ab than in nontreated NOD-*scid* mice (15–17). These results suggest that NK cells contribute to rejection of the transplanted xenograft. Conversely, our previous experiments have suggested that dendritic cells (DCs) might have a more pivotal role in xenograft rejection than NK cells. In our experiments, we found that the xenoengraftment level was significantly suppressed in NOD-*scid* mice treated with anti-NK Abs compared with NOG mice (6). Furthermore, we revealed that the production of inflammatory cytokines, such as IFN-γ and IL-6, was markedly reduced by spleen cells from NOG mice and CD11c$^+$ DC-depleted NOD-*scid* mice but not by those from NK cell-depleted NOD-*scid* mice (6). These results imply that the dysfunction of CD11c$^+$ DCs in NOG mice may be related to the high efficacy of xenoengraftment in these mice.

*Central Institute for Experimental Animals, Kawasaki-ku, Kawasaki, Kanagawa 210-0821, Japan; and †Department of Anatomy, Keio University School of Medicine, Shinjuku-ku, Tokyo 160-8582, Japan

Received for publication March 13, 2012. Accepted for publication August 29, 2012.

This work was supported by the Keio University Grant-in-Aid for Encouragement of Young Medical Scientists from Keio University School of Medicine and by a Grant-in-Aid for Young Scientists (B) (22700458) and for Scientific Research (S) (18100005) from the Ministry of Education, Culture, Sports, Science and Technology, Japan.

Address correspondence and reprint requests to Dr. Mamoru Ito, Central Institute for Experimental Animals, 3-25-12 Tonomachi, Kawasaki-ku, Kawasaki, Kanagawa 210-0821, Japan. E-mail address: mito@ciea.or.jp

The online version of this article contains supplemental material.

Abbreviations used in this article: BM, bone marrow; CIEA, Central Institute for Experimental Animals; DC, dendritic cell; hPBMC, human PBMC; HSC, hematopoietic stem cell; IKDC, IFN-producing killer dendritic cell; KO, knockout; mDC, myeloid dendritic cell; MNC, mononuclear cell; NOG, NOD/Shi-*scid*-IL2rγ^{null}; PB, peripheral blood; pDC, plasmacytoid dendritic cell; PI, propidium iodide; SIRP-α, signal regulatory protein-α.

www.jimmunol.org/cgi/doi/10.4049/jimmunol.1200820

DCs contribute to innate and adaptive immunity and act as professional APCs that are capable of Ag uptake, processing, and presentation to naive T cells (18, 19). DCs are classified into several populations based on surface markers and functional properties (20). Plasmacytoid dendritic cells (pDCs), characterized by the expression of CD11c and B220, represent a rare population of DCs that exists mainly in lymphoid tissues and plays a crucial role in producing type I IFNs against viruses via TLRs (21, 22). In transplant studies, prominent roles of DCs in graft rejection have been demonstrated using DC-depleted hosts (23). Thus, DCs may also suppress the reconstitution of donor cells and contribute to xenograft rejection.

In the current study, we investigated the role of DC subsets in hPBMC xenograft rejection using NOG mice. We performed transfer experiments with DC subpopulations and NK cells and demonstrated that $CD11c^+B220^+CD122^+$ cells, but not other DC subpopulations and NK cells obtained from NOD-*scid* mice, are potent inhibitors of hPBMC engraftment in NOG mice.

Materials and Methods

Ethics statement

All animal experiments were approved by the Institutional Animal Care and Use Committee of the Central Institute for Experimental Animals (CIEA) (certification number 11004A, February 16, 2011) and were performed in accordance with guidelines set forth by CIEA.

All experiments using human resources were approved by the Institutional Ethical Committee of the CIEA (certification number 08-11, September 4, 2008) and performed in accordance with CIEA guidelines. Written informed consent was obtained from all subjects in the current study.

Mice

NOD/Shi-*scid*-IL2rγ^{null} (NOG; formal name, NOD.Cg-*prkdc*^{scid}*il2rg*^{tm1Sug}/Jic) mice were bred and maintained under specific pathogen-free conditions at the CIEA. NOD.CB17-*prkdc*^{scid}/ShiJic (NOD-*scid*) mice were purchased from Clea Japan (Tokyo, Japan). NOD-*scid* EGFP transgenic mice were established by backcross mating of NOG-EGFP transgenic mice (24) to NOD-*scid* mice. IFN-γ knockout (KO) mice were kindly provided by Dr. Y. Iwakura (The University of Tokyo, Tokyo, Japan) and backcrossed with NOD-*scid* mice to establish the NOD-*scid* IFN-γ KO mice. These mice were housed in sterilized cages and fed sterilized food and water ad libitum. These four strains of immunodeficient mice were used at the age of 8–12 wk.

Transplantation of hPBMCs

Human peripheral blood (PB) samples were obtained from healthy volunteers after acquiring their informed consent. hPBMCs were isolated by Ficoll-Hypaque (GE Healthcare, Little Chalfont, Buckinghamshire, U.K.) density centrifugation and washed with PBS. Cells were resuspended in PBS and transplanted via the tail vein into NOG mice.

Isolation and transplantation of DC subpopulations and NK cells

The method used for isolating DC subpopulations has been described previously (25). Briefly, spleens from NOD-*scid*, NOG, or NOD-*scid* IFN-γ KO mice were minced and digested with 0.1% collagenase (Roche Diagnostics, Laval, QC, Canada) and DNase (1 mg/ml; Sigma-Aldrich, St. Louis, MO) at 37°C for 30 min. After washing with 2% FCS in PBS, the RBCs were lysed in Pharm Lyse buffer (BD Biosciences, San Jose, CA), and cells were stained with biotinylated mouse B220 Ab (BioLegend, San Diego, CA). To isolate DC subpopulations, cells were incubated with anti-biotin magnetic beads (Miltenyi Biotec, Sunnyvale, CA), and the $B220^+$ and $B220^-$ fractions were separated on a MACS column (Miltenyi Biotec). For myeloid dendritic cell (mDC) and pDC fractionation, the $B220^-$ cells were further reacted with anti-mouse CD11c magnetic beads (Miltenyi Biotec), and $CD11c^+$ cells were separated on a MACS column. The enriched $B220^+$ cells were almost all $CD11c^+$, as these mice lack B cells. For pDC and $CD11c^+B220^+CD122^+$ cell purification, the enriched $B220^+$ fractions were stained with PE-labeled mouse CD11c Ab (BioLegend), PE–Cy7–labeled streptavidin (BioLegend), and FITC-labeled mouse CD122 Ab (BD Biosciences). The $CD11c^+B220^+CD122^+$ cells and $CD11c^+B220^+CD122^-$ pDCs were sorted using the MoFlo cell sorter (Beckman Coulter, Stanford, CA), and the results were analyzed using FlowJo software (Tomy Digital Biology, Tokyo, Japan). The purity levels of the isolated mDC and pDC fractions ranged from 91 to 95% (MACS sorting), and those of the isolated pDCs and $CD11c^+B220^+CD122^+$ cells ranged from 97 to 99% (MoFlo sorting). NK cells, which were designated as $CD11c^-B220^-CD122^+$ cells, were isolated from the $B220^-$ cell fraction at >97% purity using the MoFlo cell sorter.

The purified mDCs, pDCs, $CD11c^+B220^+CD122^+$ cells, and NK cells were resuspended in PBS, and 1×10^5 to 2×10^5 cells were transplanted intravenously into NOG mice 1 d before hPBMC transplantation.

Flow cytometry

Bone marrow (BM), PB, and spleen samples were obtained from mice 2–7 wk after transplantation with hPBMCs. RBCs were lysed using the Pharm Lyse buffer (BD Biosciences), and mononuclear cells (MNCs) were prepared as single-cell suspensions. MNCs were incubated for 30 min at 4°C in the dark with the appropriate Abs. The following Abs were used: allophycocyanin–Cy7–labeled human CD45, PE- and allophycocyanin-labeled mouse CD11c, PE–Cy7–labeled mouse B220, PE-labeled mouse Siglec-H, PDCA-1, and Ly49D, and allophycocyanin-labeled mouse DX5 (BioLegend). After washing with 2% FCS in PBS, the MNCs were suspended in propidium iodide (PI) solution (BD Biosciences), followed by multicolor flow cytometry (FACSCanto; BD Biosciences) and analysis of the results using FACSDiva software (BD Biosciences). The rates of human leukocyte engraftment are expressed as the percentage of human $CD45^+$ ($hCD45^+$) cells in the PI^- total MNC population.

Cytotoxicity measurements

Cytotoxic activity was examined using the [^{51}Cr] release cytotoxic assay with Yac-1 target cells (kindly provided by Dr. K. Takeda, Juntendo University, Tokyo, Japan), according to the methods described by Shultz et al. (14). Briefly, NOD-*scid*, nontransplanted NOG mice, and NOG mice transplanted with pDCs or mDCs from NOD-*scid* mice were i.p. inoculated with polyinosinic-polycytidylic acid (Sigma-Aldrich) 48 h before assaying. Splenic MNCs from these mice were cocultured with ^{51}Cr-labeled Yac-1 target cells for 4 h at 37°C in a 5% CO_2 incubator with various E:T cell ratios. Each sample was prepared in triplicate, and the culture supernatants harvested from each well were assayed in a γ-counter (ARC300; Aloka, Tokyo, Japan). The percentage specific [^{51}Cr] release was calculated using the formula: percentage specific release = $[(X - S)/(T - S)] \times 100$, where X is the mean experimental release of [^{51}Cr] measured in triplicate wells. Total release (T) was determined from wells with ^{51}Cr-labeled Yac-1 cells and 1 N HCl, and spontaneous release (S) was determined from wells with ^{51}Cr-labeled Yac-1 cells and medium.

Induction of IFN-γ from DCs in vitro

In vitro IFN-γ induction was determined according to the methods described by Vremec et al. (25). Briefly, magnetically sorted pDC and mDC fractions were cultured in RPMI 1640 medium (Invitrogen, Carlsbad, CA) that contained 10% FCS in 96-well flat-bottom plates at 37°C in 5% CO_2. To induce IFN-γ, cells were stimulated with 5 ng/ml IL-12p70 (R&D Systems, Minneapolis, MN) and 20 ng/ml IL-18 (R&D Systems) or with 10 ng/ml PMA (Sigma-Aldrich) and 1 μg/ml ionomycin (Sigma-Aldrich) for 48 h. Culture supernatants were collected and stored at −80°C until use. IFN-γ was assayed using the Mouse IFNγ Quantikine ELISA Kit (R&D Systems).

Morphological analysis

pDCs, $CD11c^+B220^+CD122^+$ cells, and NK cells were isolated as described earlier. For May–Grünwald Giemsa staining, the enriched subpopulations were precipitated onto silane-coated glass slides (Muto Pure Chemicals, Tokyo, Japan) by cytospinning and were then air dried for 3 min. The slides were soaked in May–Grünwald solution (Muto Pure Chemicals) for 3 min and washed under running water to remove extra stain. The slides were further stained with 0.5% Giemsa solution (Muto Pure Chemicals) for 15 min. After washing with running water, the slides were dried and subjected to microscopic analyses.

Area and perimeter measurements of these smeared cells were automatically calculated using ImageJ 1.45s software (National Institutes of Health, Bethesda, MD).

Statistical analysis

Mean values and standard deviations were computed using Excel (Microsoft, Redmond, WA). Significant differences were calculated by Student t tests

and shown as $*p < 0.05$ and $**p < 0.005$. A p value <0.05 was deemed to be statistically significant.

Results

Suppression of human cell engraftment by the CD11c$^+$B220$^+$ pDC fraction

To investigate the effects of DCs on xenograft rejection, we first isolated two distinct DC fractions, CD11c$^+$B220$^+$ (pDCs) and CD11c$^+$B220$^-$ (mDCs), from NOD-*scid* and NOG mice, respectively. These two DC fractions were intravenously transplanted into NOG mice before hPBMC transplantation (Fig. 1A). The efficacy of successful hPBMC engraftment in PB, BM, and spleens from NOG DC-transplanted NOG mice and NOD-*scid* mDC-transplanted NOG mice was at the same level as that of non-transplanted control NOG mice. In contrast, hPBMC engraftment was completely suppressed in the PB, BM, and spleens of NOD-*scid* pDC-transplanted NOG mice at 7 wk posttransplantation (Fig. 1B). Spleen cells from the NOD-*scid*, NOD-*scid* pDC-transplanted or mDC-transplanted NOG, and untreated NOG mice without hPBMC transplantation were cocultured with Yac-1 target cells that were labeled with [^{51}Cr], then [^{51}Cr] release into the culture supernatants was measured. Although cytotoxicity was less effective compared with spleen cells of NOD-*scid* mice, those from the pDC-transplanted NOG mice showed a higher level of cytotoxicity compared with mDC-transplanted NOG and non-transplanted NOG mice (Fig. 1C). These results show that the high level of engraftment of NOG mice is suppressed by the NOD-*scid* pDC fraction, indicating that this fraction includes cells that mediate xenograft rejection.

NK marker-expressed cells in the pDC fraction have the potential for xenograft rejection

To identify cells that play critical roles in graft rejection, we used NOD-*scid* mice that systemically expressed GFP (NOD-*scid* EGFP Tg), and transplanted the pDC and mDC fractions isolated from the mice into NOG mice before hPBMC transplantation. At 7 wk posttransplantation, engraftment of hCD45$^+$ cells was inhibited in BM and spleens of the pDC-transplanted NOG mice (Fig. 2A, *top left panel*), consistent with the results shown in Fig. 1B. Also, GFP$^+$ cells were detected in the spleens of the pDC-transplanted NOG mice but not in those of the mDC-transplanted NOG mice (Fig. 2A, *top right panel*), and these GFP$^+$ cells expressed the DX5 Ag (Fig. 2A, *bottom panel*). These GFP$^+$DX5$^+$ cells might be expanded by recognizing xenografts and are considered to be responsible for their rejection. CD11c$^+$B220$^+$DX5$^+$ cells are known to produce high levels of IFN-γ upon stimulation (26, 27). We compared the levels of IFN-γ production of the isolated DC subpopulations from the spleen cells of NOD-*scid* and NOG mice. After stimulation with either IL-12 plus IL-18 or PMA plus ionomycin, high-level production of IFN-γ was observed in the pDCs from the NOD-*scid* mice but not in those from the NOG mice (Fig. 2B). We compared the expression of Siglec-H, PDCA-1, and CD122 on CD11c$^+$B220$^+$ cells between NOD-*scid* and NOG mice. pDCs generally express Siglec-H and PDCA-1 (28, 29) but not CD122, which is an NK cell marker and often used for detection of DX5 (30). Siglec-H and PDCA-1 were expressed on all CD11c$^+$B220$^+$ cells in the spleen of NOG mice, but CD122$^+$ cells were not observed (Fig. 2C). However, ~30% of CD11c$^+$B220$^+$CD122$^+$ cells were present in the spleens of NOD-*scid*

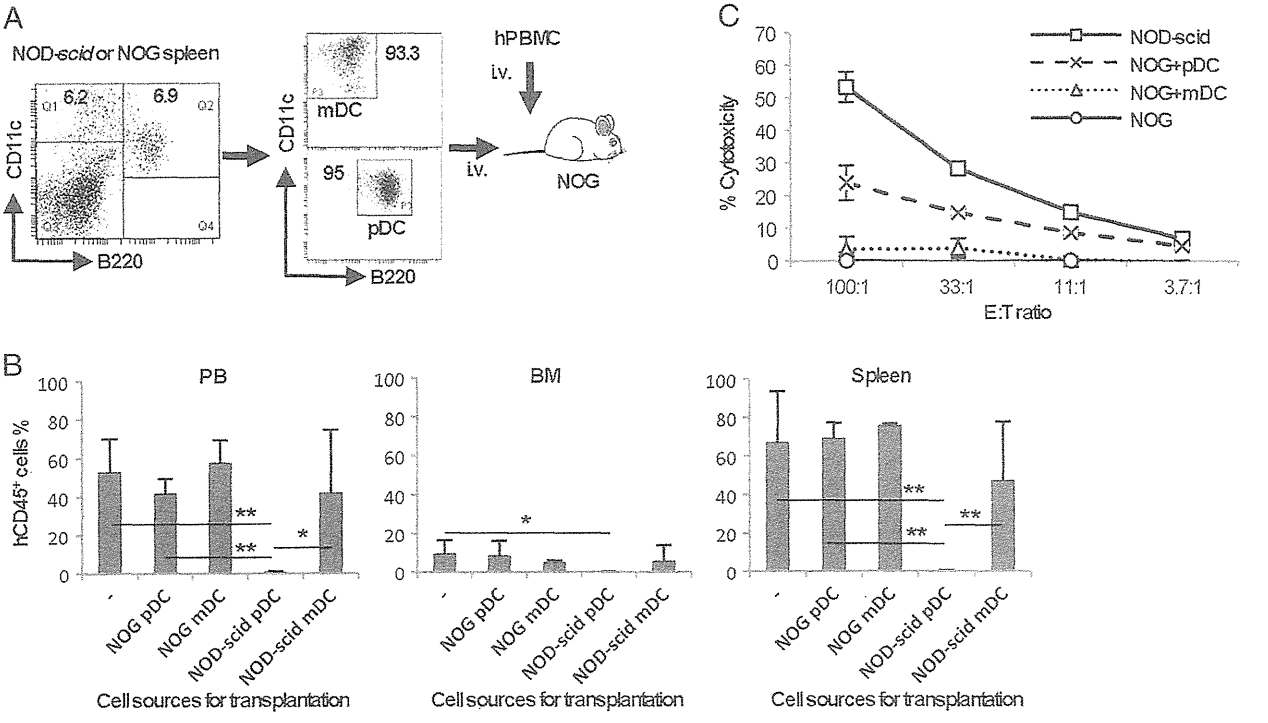

FIGURE 1. Suppression of xenoengraftment by the pDC fraction. (**A**) CD11c$^+$B220$^+$ pDCs and CD11c$^+$B220$^-$ mDCs from the spleens of NOD-*scid* and NOG mice were isolated using magnetic beads and MACS columns. These DC fractions (2×10^5 cells) were intravenously transplanted into NOG mice. At 1–2 d posttransplantation of the pDC or mDC fraction, 5×10^6 hPBMCs were intravenously transplanted into the NOG mice. (**B**) Engraftment of hCD45$^+$ cells is significantly inhibited in the PB, BM, and spleens of NOD-*scid* pDC-transplanted NOG mice ($n = 5$) but not in the PB, BM, and spleens of mDC-transplanted NOG mice ($n = 4$), and engraftment is not inhibited in nontreated NOG mice ($n = 3$) and NOG DC-transplanted NOG mice ($n = 3$) at 7 wk after hPBMC transplantation. (**C**) Spleen cells from NOD-*scid* (square plot), NOD-*scid* pDC-transplanted (cross plot), or mDC-transplanted (triangle plot) NOG mice and from untreated NOG mice (circle plot) were cocultured in triplicate with ^{51}Cr-labeled Yac-1 cells at various ratios for 4 h. Spleen cells from pDC-transplanted NOG mice showed high cytotoxicity compared with those from mDC-transplanted NOG mice. $*p < 0.05$, $**p < 0.005$.

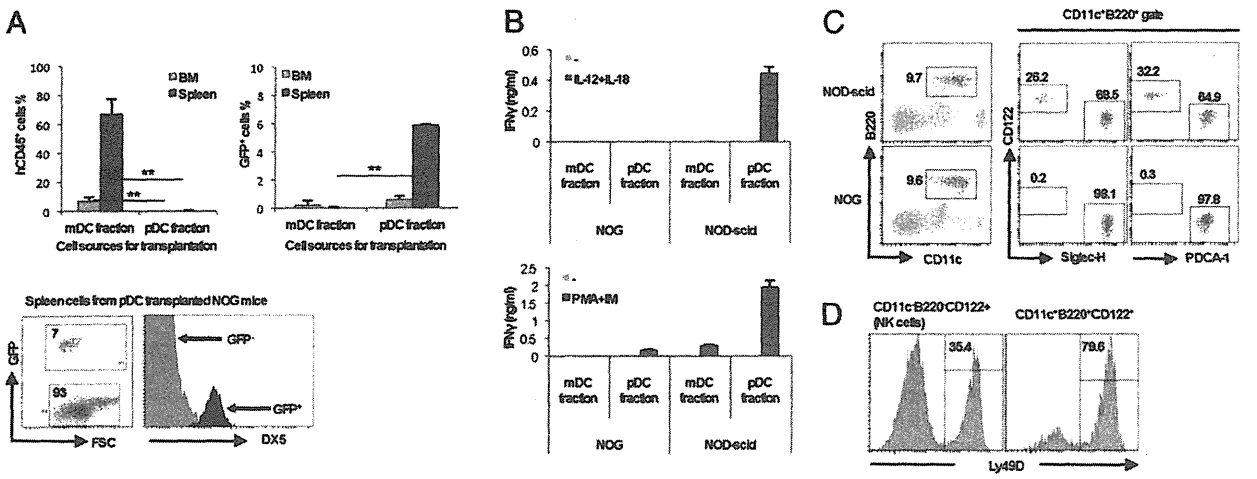

FIGURE 2. NK marker-expressed cells in the pDC fraction have the potential for xenograft rejection. (**A**) The pDC or mDC fraction from NOD-*scid* EGFP Tg mice was transplanted (2×10^5 cells) into NOG mice prior to transplantation with 5×10^6 hPBMCs, and the engrafted human cells and transplanted GFP^+ mouse cells were analyzed by flow cytometry at 7 wk posttransplantation. Engraftment of $hCD45^+$ cells was evident in the mDC-transplanted NOG mice ($n = 3$) but not in the pDC-transplanted NOG mice ($n = 3$). The percentage of engrafted mouse cells that expressed GFP was higher in the pDC-transplanted NOG mice than in the mDC-transplanted NOG mice. All the engrafted GFP^+ cells expressed the DX5 Ag. (**B**) The mDC or pDC fraction was isolated from NOD-*scid* or NOG mice, and 1×10^5 cells were cultured in duplicate with or without IL-12 plus IL-18 (*upper panel*) or PMA plus ionomycin (PMA+IM; *lower panel*). IFN-γ was strongly produced from the NOD-*scid* pDC fraction stimulated under both culture conditions. These assays were performed simultaneously, and the results are representative of three independent experiments. (**C**) Spleen cells from NOD-*scid* or NOG mice were stained with CD11c, B220, CD122, and Siglec-H or PDCA-1 Abs and analyzed by flow cytometry. $CD122^+$Siglec-H^- or $CD122^+PDCA\text{-}1^-$ cells were detected in the NOD-*scid* pDC fraction but not in the NOG pDC fraction. (**D**) Spleen cells from NOD-*scid* mice were stained with CD11c, B220, CD122, and Ly49D Abs. The histogram shows the frequencies of Ly49D expression on $CD11c^-B220^-CD122^+$ NK cells (*left*) and on $CD11c^+B220^+CD122^+$ cells (*right*). Similar results were obtained in three independent experiments (C, D). $^{**}p < 0.005$.

mice. We further analyzed Ly49D expression on $CD11c^+B220^+CD122^+$ cells in NOD-*scid* mice. Ly49D is a receptor on NK cells and mediates allograft rejection by recognition of MHC class I molecules (31, 32). The frequency of Ly49D expression on $CD11c^+B220^+CD122^+$ cells was higher compared with that on $CD11c^-B220^-CD122^+$ NK cells in the spleens of NOD-*scid* mice (Fig. 2D). These results suggest that $CD11c^+B220^+CD122^+$ cells have a high potency for xenograft rejection and their absence in NOG mice may lead to high-level engraftment of human cells.

$CD11c^+B220^+CD122^+$ cells suppress xenoengraftment in NOG mice

To determine whether $CD11c^+B220^+CD122^+$ cells inhibit the engraftment of human cells, we isolated $CD11c^+B220^+CD122^+$ cells or pDCs ($CD11c^+B220^+CD122^-$) from NOD-*scid* mice by cell sorting (Fig. 3A). It is well known that pDCs produce type I IFNs after treatment with a TLR9 ligand (25). We demonstrated that isolated pDCs could produce IFN-α; however, IFN-α was not produced by $CD11c^+B220^+CD122^+$ cells (Supplemental Fig. 1). $CD11c^+B220^+CD122^+$ cells or pDCs were transplanted into NOG mice prior to hPBMC transplantation (Fig. 3A). Engraftment of the $hCD45^+$ leukocytes was significantly suppressed in the PB, BM, and spleens of $CD11c^+B220^+CD122^+$ cell-transplanted NOG mice, whereas the pDC-transplanted NOG mice showed similar percentages of engrafted human leukocytes to the non-transplanted control NOG mice at 7 wk posttransplantation with hPBMCs (Fig. 3B). We also isolated pDCs or $CD11c^+B220^+CD122^+$ cells from NOD-*scid* and NOD-*scid* IFN-γ KO mice and transplanted them into NOG mice. The percentages of engrafted human leukocytes in the PB, BM, and spleens were not reduced by $CD11c^+B220^+CD122^+$ cells from NOD-*scid* IFN-γ KO mice (Fig. 3C). These results revealed that $CD11c^+B220^+CD122^+$ cells play a crucial role in xenograft rejection via IFN-γ production.

Suppressive effects of $CD11c^+B220^+CD122^+$ cells and NK cells on xenoengraftment

The possible involvement of NK cells in xenograft rejection was examined because these cells produce IFN-γ and are defective in NOG mice. Thus, we compared the efficiencies of xenograft rejection for $CD11c^+B220^+CD122^+$ cells and $CD11c^-B220^-CD122^+$ NK cells. $CD11c^+B220^+CD122^+$ cells and NK cells were sorted from the spleen cells of NOD-*scid* mice and intravenously transplanted (1×10^5 or 2×10^5 cells) into NOG mice before hPBMC transplantation (Fig. 4A). At 2 and 4 wk posttransplantation, the $CD11c^+B220^+CD122^+$ cells were found to suppress human cell engraftment more potently than NK cells when 2×10^5 cells were transplanted (Fig. 4B, *right panel*), although the $CD11c^+B220^+CD122^+$ cells and NK cells did not cause rejection when 1×10^5 cells were transplanted (Fig. 4B, *left panel*). In vitro cytotoxic assays showed that the killing activity of $CD11c^+B220^+CD122^+$ cells was slightly higher than that of NK cells and that it could be suppressed by treating cells with an anti-NKG2D blocking Ab (Supplemental Fig. 2). Overall, these results indicate that $CD11c^+B220^+CD122^+$ cells have a greater potential than NK cells to induce xenograft rejection.

$CD11c^+B220^+CD122^+$ cells are distinguishable from NK cells

Previously, Vosshenrich et al. (33) reported that B220 expression on NK cells was inducible after activation in vitro and in vivo, and they argued that activated NK cells show a phenotypic resemblance to the $CD11c^+B220^+CD122^+$ IFN-producing killer dendritic cells (IKDCs). In contrast, Guimont-Desrochers et al. (34) showed that NK cells did not acquire B220 expression after adoptive transfer. To clarify this inconsistency, we investigated whether the sorted NK cells upregulated B220 and CD11c molecules after adoptive transfer. Fig. 5A shows that transplanted $CD122^+$ cells did not acquire B220 expression in the spleens of NK cell-transplanted NOG mice, whereas a small amount of

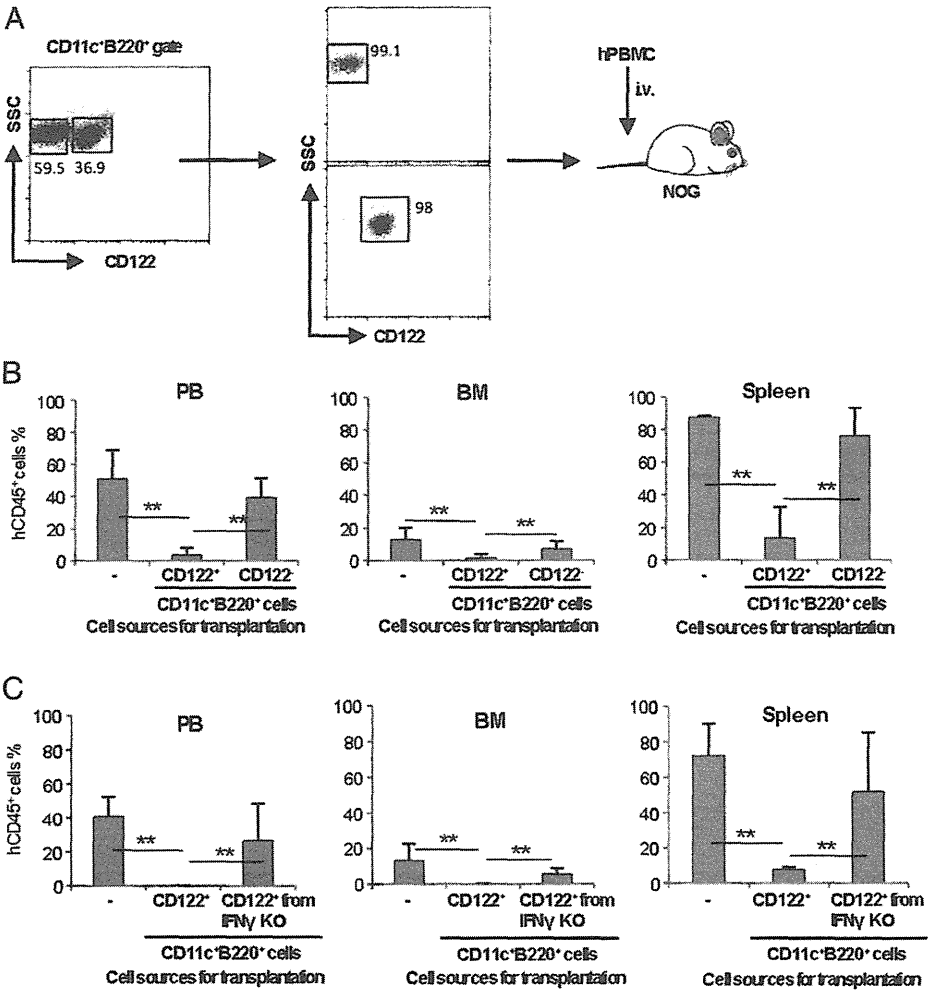

FIGURE 3. $CD11c^+B220^+CD122^+$ cells, but not pDCs, suppress xenoengraftment. (**A**) Scheme for the isolation of pDCs or $CD11c^+B220^+CD122^+$ cells using a MoFlo cell sorter and subsequent cell transfer (2×10^5 cells) into NOG mice before transplantation of hPBMCs (5×10^6 cells). (**B**) $hCD45^+$ human cell engraftment was analyzed by flow cytometry in the PB, BM, and spleens at 7 wk after hPBMC transplantation. The pDC-transplanted NOG mice ($n = 5$) showed a similar engraftment rate to that of the nontreated NOG ($n = 3$) mice, whereas a remarkable decrease in human cell engraftment was observed in the $CD11c^+B220^+CD122^+$ cell-transplanted NOG mice ($n = 5$). (**C**) $CD11c^+B220^+CD122^+$ cells from NOD-*scid* or NOD-*scid* IFN-γ KO mice were isolated and transplanted (2×10^5 cells) into NOG mice, followed by transplantation of 5×10^6 hPBMCs. The percentages of engrafted leukocytes were analyzed by flow cytometry at 6 wk posttransplantation. The percentage of $hCD45^+$ cells was inhibited in the PB, BM, and spleens of the NOD-*scid* $CD11c^+B220^+CD122^+$ cell-transplanted NOG mice ($n = 11$), whereas IFN-γ KO $CD11c^+B220^+CD122^+$ cells did not inhibit $hCD45^+$ cells as well as nontransplanted control NOG mice ($n = 6$). $^{**}p < 0.005$.

$CD122^+$ cells simultaneously expressed B220 and CD11c molecules in the spleens of $CD11c^+B220^+CD122^+$ cell-transplanted NOG mice. We further analyzed the morphological differences among sorted $CD11c^+B220^+CD122^+$ cells, NK cells, and pDCs by May–Giemsa staining. As observed in Fig. 5B, $CD11c^+B220^+CD122^+$ cells resembled pDCs; they showed a monocytic mor-

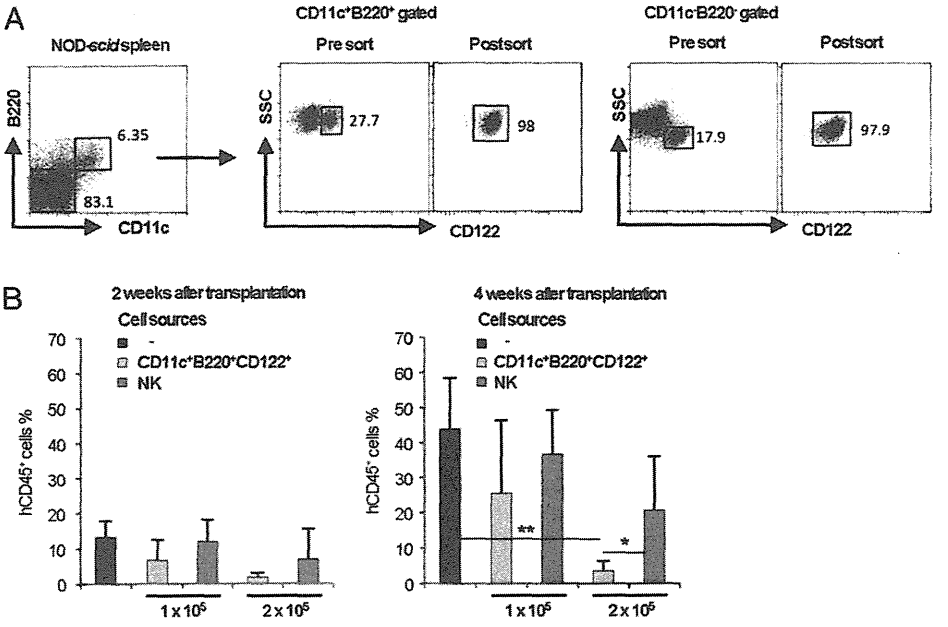

FIGURE 4. Suppressive effects of $CD11c^+B220^+CD122^+$ and NK cells on xenoengraftment. (**A**) $CD11c^+B220^+CD122^+$ cells or NK cells were positively isolated from the $CD11c^+B220^+$ fraction or $CD11c^-B220^-$ fraction of NOD-*scid* mice spleen cells using the MoFlo cell sorter, and 1×10^5 or 2×10^5 cells were transplanted into NOG mice before hPBMC transplantation. (**B**) At 2 and 4 wk posttransplantation, RBC-lysed PBMCs were collected from the transplanted NOG mice, and the efficacy of human cell engraftment was analyzed by flow cytometry. The percentage of engrafted $hCD45^+$ cells was significantly lower in the 2×10^5 $CD11c^+B220^+CD122^+$ cell-transplanted NOG mice ($n = 6$) than in the 2×10^5 NK cell-transplanted mice ($n = 7$). $^*p < 0.05$, $^{**}p < 0.005$.

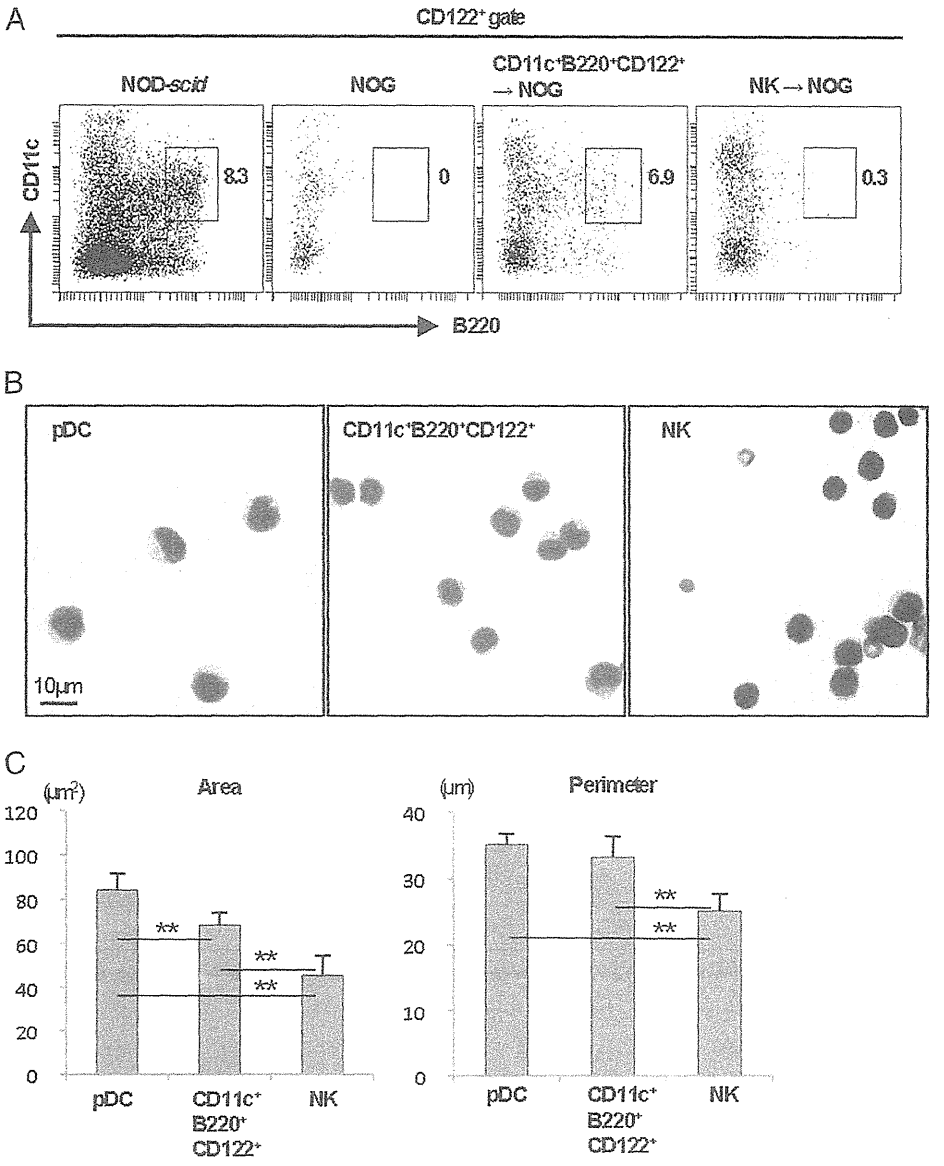

FIGURE 5. $CD11c^+B220^+CD122^+$ cells are distinguishable from NK cells. (**A**) $CD11c^+B220^+CD122^+$ or NK cells were purified using a MoFlo cell sorter, and 1×10^5 of these cells was transplanted into NOG mice. Two weeks after transplantation, spleen cells from the transplanted NOG, NOD-*scid*, and NOG mice were analyzed by flow cytometry. (**B**) Morphology of $CD11c^+B220^+CD122^+$ cells. Cytospin samples of sorted pDCs, $CD11c^+B220^+CD122^+$ cells, and NK cells were stained by May–Giemsa. (**C**) The means of the areas and perimeters of pDCs, $CD11c^+B220^+CD122^+$ cells, and NK cells were calculated using the ImageJ software. Similar results were obtained in two independent experiments. $^{**}p < 0.005$.

phology, low nuclear/cytoplasmic ratio, and dispersed chromatin. In contrast, NK cells showed a lymphocytic morphology, high nuclear/cytoplasmic ratio, and hyperchromatic nuclei. Moreover, we compared the area and perimeters of these cell populations using ImageJ analysis. $CD11c^+B220^+CD122^+$ cells had an intermediate area size between that of pDCs and NK cells and a larger perimeter than NK cells (Fig. 5C). These results demonstrated that $CD11c^+B220^+CD122^+$ cells were phenotypically and morphologically distinct from NK cells.

Discussion

In the current study, we investigated the mechanism underlying the high acceptance rate of xenografts in NOG mice. To determine the cells responsible for xenograft rejection, we transplanted DC subpopulations and NK cells from NOD-*scid* mice into NOG mice. We showed that the $CD11c^+B220^+CD122^+$ cells from NOD-*scid* mice strongly inhibited the engraftment of transplanted hPBMCs, whereas other DC subpopulations and NK cells from NOD-*scid* mice did not highly contribute to xenograft rejection in NOG mice. Throughout these experiments, we revealed that $CD11c^+B220^+CD122^+$ cells with characteristics commonly shared by IKDCs and activated NK cells—which are controversial cell lineages in xenograft rejection—are responsible for the rejection in immunodeficient mice.

A DC subpopulation that expresses NK cell markers CD122 and DX5 in the pDC fraction was identified as IKDCs, which share the functional properties and surface markers of DCs and NK cells and have cytotoxic activities and Ag-presenting abilities (35, 36). Taieb et al. (36) reported that IKDCs prevented transplanted tumor outgrowth and that IFN-γ–dependent and TRAIL-dependent killing activities and tumor recognition via MHC class II molecules occurred simultaneously when these cells were adoptively transferred, whereas conventional NK cells did not prevent these events. The authors claimed that IKDCs participate in tumor surveillance and act as effectors of innate immune responses. Regarding activated NK cells, $CD11c^+B220^+CD122^+$ cells more closely resemble NK cells than DCs (33, 37–39) because their developmental pathway is very similar to that of NK cells that rely on IL-15 signaling through the IL-2Rβ, IL-15Rβ, and common γ-chain. In our results, the $CD11c^+B220^+CD122^+$ cells resembled activated NK cells but not pDCs, as $CD11c^+B220^+CD122^+$ cells did not express Siglec-H and PDCA-1 and did not produce IFN-α

after TLR9 stimulation, and cytotoxicity was suppressed by NKG2D Ab treatment. These results were consistent with activated NK cells reported by Blasius et al. (39). However, $CD11c^+B220^+CD122^+$ cells were morphologically distinct from NK cells, and NK cells did not acquire B220 expression after adoptive transfer. Recently, Guimont-Desrochers et al. (34) obtained similar results demonstrating that $CD11c^+B220^+CD122^+$ cells are distinct from activated NK cells. Thus, controversy remains in describing the relationship between $CD11c^+B220^+CD122^+$ cells and activated NK cells, and further studies are needed to define the differences between these cells.

The role of NK cells in xenograft rejection in NOD-*scid* mice has been described previously. Kollet et al. (15) reported an 11-fold higher rate of xenoengraftment after transplantation of human HSCs for NOD-*scid* $\beta2m^{null}$ mice that lacked NK activity compared with that for NOD-*scid* mice. Additionally, McKenzie et al. (17) showed enhancement of xenoengraftment after HSC transplantation when the NK cells were eliminated by treatment with a CD122 Ab. In those studies, the observed higher xenoengraftment level cannot be attributed solely to NK cells because $CD11c^+B220^+CD122^+$ cells could have been present in their eliminated fraction. Our current results indicate that $CD11c^+B220^+CD122^+$ cells are more effective than NK cells at inducing xenograft rejection, and we conclude that $CD11c^+B220^+CD122^+$ cells, but not NK cells, are the main effector cells for xenograft rejection. $CD11c^+B220^+CD122^+$ cells produce higher levels of IFN-γ than NK cells upon IL-15 stimulation (35, 36). Chaudhry et al. (40) reported that $CD11c^+B220^+NK1.1^+$ cells (called NKDCs), which are the same as $CD11c^+B220^+CD122^+$ cells, and NK cells were absent in IL-$15^{-/-}$ mice, and they observed that $CD11c^+B220^+NK1.1^+$ cells were restored more rapidly than NK cells by exogenous IL-15 treatment. Their in vitro analysis showed that $CD11c^+B220^+NK1.1^+$ cells stimulated with IL-15 retained cytotoxic capacity and potent IFN-γ secretion. Moreover, tumor metastasis in the lung caused by transplanted B16F10 melanoma cells was inhibited by syngeneic $CD11c^+B220^+NK1.1^+$ cell transplantation. In contrast, $CD11c^+B220^+NK1.1^+$ cells from IFN-γ−deficient mice did not cause this type of inhibition. Furthermore, Lin et al. (41) transplanted pig cells into T cell-depleted, IFN-γ–deficient mice and found that the engraftment of pig cells was significantly enhanced in the IFN-γ–deficient mice compared with the control T cell-depleted, wild-type mice. Those findings support our current results that $CD11c^+B220^+CD122^+$ cells from IFN-γ–deficient mice do not suppress xenoengraftment. Thus, xenograft rejection by $CD11c^+B220^+CD122^+$ cells may depend on the amount of IFN-γ, and IFN-γ deficiency may contribute to the high acceptance rate of xenografts in NOG mice. However, we have no evidence that the IFN-γ produced by $CD11c^+B220^+CD122^+$ cells modulates the rejection of xenografts. We speculate that IFN-γ can promote xenograft rejection through at least two scenarios. In the first scenario, $CD11c^+B220^+CD122^+$ cells self-activate in an autocrine manner through secretion of IFN-γ and enhance cytotoxicity mediated by perforin/granzyme, FasL, and the TRAIL pathway against targeted xenografts that lack species-specific MHC class I molecules, which interact with killer inhibitory receptors (42). In the second scenario, IFN-γ produced by $CD11c^+B220^+CD122^+$ cells induces the activation of macrophages, and these macrophages are subsequently recruited to the graft site through the upregulation of monocyte-attracting chemokines, resulting in a direct attack on the xenograft. The relative importance of IFN-γ–dependent xenograft rejection by $CD11c^+B220^+CD122^+$ cells remains to be elucidated.

In conclusion, we demonstrated that the high-level acceptance of xenografts in NOG mice is due to a lack of $CD11c^+B220^+CD122^+$ cells, and we suggest that IFN-γ produced by $CD11c^+B220^+CD122^+$ cells plays an important role in xenograft rejection. These data are useful for clarifying the immunological mechanisms leading to rejection of xenotransplants. Further studies are needed to confirm the exact pathway involved in $CD11c^+B220^+CD122^+$ cell-dependent mechanisms of xenograft rejection.

Acknowledgments

We thank Masaki Terabe of the National Cancer Institute for valuable advice, Masashi Sasaki of JAC, Inc. for technical assistance, and Yasuhiko Ando and Nagisa Ogata of JAC, Inc. for animal care.

Disclosures

The authors have no financial conflicts of interest.

References

1. Suemizu, H., M. Hasegawa, K. Kawai, K. Taniguchi, M. Monnai, M. Wakui, M. Suematsu, M. Ito, G. Peltz, and M. Nakamura. 2008. Establishment of a humanized model of liver using NOD/Shi-scid IL2Rgnull mice. *Biochem. Biophys. Res. Commun.* 377: 248–252.
2. Terada, Y., Y. Terunuma-Sato, T. Kakoi-Yoshimoto, H. Hasegawa, T. Ugajin, Y. Koyanagi, M. Ito, T. Murakami, H. Sasano, N. Yaegashi, and K. Okamura. 2008. Development of human Graafian follicles following transplantation of human ovarian tissue into NOD/SCID/gammac null mice. *Am. J. Reprod. Immunol.* 60: 534–540.
3. Suemizu, H., M. Monnai, Y. Ohnishi, M. Ito, N. Tamaoki, and M. Nakamura. 2007. Identification of a key molecular regulator of liver metastasis in human pancreatic carcinoma using a novel quantitative model of metastasis in NOD/SCID/gammacnull (NOG) mice. *Int. J. Oncol.* 31: 741–751.
4. Miyakawa, Y., Y. Ohnishi, M. Tomisawa, M. Monnai, K. Kohmura, Y. Ueyama, M. Ito, Y. Ikeda, M. Kizaki, and M. Nakamura. 2004. Establishment of a new model of human multiple myeloma using NOD/SCID/gammac(null) (NOG) mice. *Biochem. Biophys. Res. Commun.* 313: 258–262.
5. Ito, R., I. Katano, K. Kawai, H. Hirata, T. Ogura, T. Kamisako, T. Eto, and M. Ito. 2009. Highly sensitive model for xenogenic GVHD using severe immunodeficient NOG mice. *Transplantation* 87: 1654–1658.
6. Ito, M., H. Hiramatsu, K. Kobayashi, K. Suzue, M. Kawahata, K. Hioki, Y. Ueyama, Y. Koyanagi, K. Sugamura, K. Tsuji, et al. 2002. NOD/SCID/gamma (c)(null) mouse: an excellent recipient mouse model for engraftment of human cells. *Blood* 100: 3175–3182.
7. Hiramatsu, H., R. Nishikomori, T. Heike, M. Ito, K. Kobayashi, K. Katamura, and T. Nakahata. 2003. Complete reconstitution of human lymphocytes from cord blood CD34+ cells using the NOD/SCID/gammacnull mice model. *Blood* 102: 873–880.
8. Bosma, G. C., R. P. Custer, and M. J. Bosma. 1983. A severe combined immunodeficiency mutation in the mouse. *Nature* 301: 527–530.
9. Ohbo, K., T. Suda, M. Hashiyama, A. Mantani, M. Ikebe, K. Miyakawa, M. Moriyama, M. Nakamura, M. Katsuki, K. Takahashi, et al. 1996. Modulation of hematopoiesis in mice with a truncated mutant of the interleukin-2 receptor gamma chain. *Blood* 87: 956–967.
10. Wang, H., M. L. Madariaga, S. Wang, N. Van Rooijen, P. A. Oldenborg, and Y. G. Yang. 2007. Lack of CD47 on nonhematopoietic cells induces split macrophage tolerance to CD47null cells. *Proc. Natl. Acad. Sci. USA* 104: 13744–13749.
11. Ide, K., H. Wang, H. Tahara, J. Liu, X. Wang, T. Asahara, M. Sykes, Y. G. Yang, and H. Ohdan. 2007. Role for CD47-SIRPalpha signaling in xenograft rejection by macrophages. *Proc. Natl. Acad. Sci. USA* 104: 5062–5066.
12. Wang, H., J. VerHalen, M. L. Madariaga, S. Xiang, S. Wang, P. Lan, P. A. Oldenborg, M. Sykes, and Y. G. Yang. 2007. Attenuation of phagocytosis of xenogeneic cells by manipulating CD47. *Blood* 109: 836–842.
13. Takenaka, K., T. K. Prasolava, J. C. Wang, S. M. Mortin-Toth, S. Khalouei, O. I. Gan, J. E. Dick, and J. S. Danska. 2007. Polymorphism in Sirpa modulates engraftment of human hematopoietic stem cells. *Nat. Immunol.* 8: 1313–1323.
14. Shultz, L. D., P. A. Schweitzer, S. W. Christianson, B. Gott, I. B. Schweitzer, B. Tennent, S. McKenna, L. Mobraaten, T. V. Rajan, D. L. Greiner, et al. 1995. Multiple defects in innate and adaptive immunologic function in NOD/LtSz-scid mice. *J. Immunol.* 154: 180–191.
15. Kollet, O., A. Peled, T. Byk, H. Ben-Hur, D. Greiner, L. Shultz, and T. Lapidot. 2000. beta2 microglobulin-deficient (B2m(null)) NOD/SCID mice are excellent recipients for studying human stem cell function. *Blood* 95: 3102–3105.
16. Glimm, H., W. Eisterer, K. Lee, J. Cashman, T. L. Holyoake, F. Nicolini, L. D. Shultz, C. von Kalle, and C. J. Eaves. 2001. Previously undetected human hematopoietic cell populations with short-term repopulating activity selectively engraft NOD/SCID-beta2 microglobulin-null mice. *J. Clin. Invest.* 107: 199–206.
17. McKenzie, J. L., O. I. Gan, M. Doedens, and J. E. Dick. 2005. Human short-term repopulating stem cells are efficiently detected following intrafemoral transplantation into NOD/SCID recipients depleted of CD122+ cells. *Blood* 106: 1259–1261.
18. Banchereau, J., and R. M. Steinman. 1998. Dendritic cells and the control of immunity. *Nature* 392: 245–252.
19. Lanzavecchia, A., and F. Sallusto. 2001. The instructive role of dendritic cells on T cell responses: lineages, plasticity and kinetics. *Curr. Opin. Immunol.* 13: 291–298.

20. Shortman, K., and S. H. Naik. 2007. Steady-state and inflammatory dendritic-cell development. *Nat. Rev. Immunol.* 7: 19–30.
21. Rothenfusser, S., E. Tuma, S. Endres, and G. Hartmann. 2002. Plasmacytoid dendritic cells: the key to CpG. *Hum. Immunol.* 63: 1111–1119.
22. Kadowaki, N., S. Ho, S. Antonenko, R. W. Malefyt, R. A. Kastelein, F. Bazan, and Y. J. Liu. 2001. Subsets of human dendritic cell precursors express different toll-like receptors and respond to different microbial antigens. *J. Exp. Med.* 194: 863–869.
23. Garrod, K. R., F. C. Liu, L. E. Forrest, I. Parker, S. M. Kang, and M. D. Cahalan. 2010. NK cell patrolling and elimination of donor-derived dendritic cells favor indirect alloreactivity. *J. Immunol.* 184: 2329–2336.
24. Suemizu, H., C. Yagihashi, T. Mizushima, T. Ogura, T. Etoh, K. Kawai, and M. Ito. 2008. Establishing EGFP congenic mice in a NOD/Shi-scid IL2Rg(null) (NOG) genetic background using a marker-assisted selection protocol (MASP). *Exp. Anim.* 57: 471–477.
25. Vremec, D., M. O'Keeffe, H. Hochrein, M. Fuchsberger, I. Caminschi, M. Lahoud, and K. Shortman. 2007. Production of interferons by dendritic cells, plasmacytoid cells, natural killer cells, and interferon-producing killer dendritic cells. *Blood* 109: 1165–1173.
26. Chaudhry, U. I., T. P. Kingham, G. Plitas, S. C. Katz, J. R. Raab, and R. P. DeMatteo. 2006. Combined stimulation with interleukin-18 and CpG induces murine natural killer dendritic cells to produce IFN-gamma and inhibit tumor growth. *Cancer Res.* 66: 10497–10504.
27. Pillarisetty, V. G., S. C. Katz, J. I. Bleier, A. B. Shah, and R. P. Dematteo. 2005. Natural killer dendritic cells have both antigen presenting and lytic function and in response to CpG produce IFN-gamma via autocrine IL-12. *J. Immunol.* 174: 2612–2618.
28. Wendland, M., N. Czeloth, N. Mach, B. Malissen, E. Kremmer, O. Pabst, and R. Förster. 2007. CCR9 is a homing receptor for plasmacytoid dendritic cells to the small intestine. *Proc. Natl. Acad. Sci. USA* 104: 6347–6352.
29. Zhang, J., A. Raper, N. Sugita, R. Hingorani, M. Salio, M. J. Palmowski, V. Cerundolo, and P. R. Crocker. 2006. Characterization of Siglec-H as a novel endocytic receptor expressed on murine plasmacytoid dendritic cell precursors. *Blood* 107: 3600–3608.
30. Guimont-Desrochers, F., Z. J. Cappello, M. Chagnon, M. McDuffie, and S. Lesage. 2009. Cutting edge: genetic characterization of IFN-producing killer dendritic cells. *J. Immunol.* 182: 5193–5197.
31. George, T. C., J. R. Ortaldo, S. Lemieux, V. Kumar, and M. Bennett. 1999. Tolerance and alloreactivity of the Ly49D subset of murine NK cells. *J. Immunol.* 163: 1859–1867.
32. Nakamura, M. C., P. A. Linnemeyer, E. C. Niemi, L. H. Mason, J. R. Ortaldo, J. C. Ryan, and W. E. Seaman. 1999. Mouse Ly-49D recognizes H-2Dd and activates natural killer cell cytotoxicity. *J. Exp. Med.* 189: 493–500.
33. Vosshenrich, C. A., S. Lesjean-Pottier, M. Hasan, O. Richard-Le Goff, E. Corcuff, O. Mandelboim, and J. P. Di Santo. 2007. CD11cloB220+ interferon-producing killer dendritic cells are activated natural killer cells. *J. Exp. Med.* 204: 2569–2578.
34. Guimont-Desrochers, F., G. Boucher, Z. Dong, M. Dupuis, A. Veillette, and S. Lesage. 2012. Redefining interferon-producing killer dendritic cells as a novel intermediate in NK-cell differentiation. *Blood* 119: 4349–4357.
35. Chan, C. W., E. Crafton, H. N. Fan, J. Flook, K. Yoshimura, M. Skarica, D. Brockstedt, T. W. Dubensky, M. F. Stins, L. L. Lanier, et al. 2006. Interferon-producing killer dendritic cells provide a link between innate and adaptive immunity. *Nat. Med.* 12: 207–213.
36. Taieb, J., N. Chaput, C. Ménard, L. Apetoh, E. Ullrich, M. Bonmort, M. Péquignot, N. Casares, M. Terme, C. Flament, et al. 2006. A novel dendritic cell subset involved in tumor immunosurveillance. *Nat. Med.* 12: 214–219.
37. Spits, H., and L. L. Lanier. 2007. Natural killer or dendritic: what's in a name? *Immunity* 26: 11–16.
38. Caminschi, I., F. Ahmet, K. Heger, J. Brady, S. L. Nutt, D. Vremec, S. Pietersz, M. H. Lahoud, L. Schofield, D. S. Hansen, et al. 2007. Putative IKDCs are functionally and developmentally similar to natural killer cells, but not to dendritic cells. *J. Exp. Med.* 204: 2579–2590.
39. Blasius, A. L., W. Barchet, M. Cella, and M. Colonna. 2007. Development and function of murine B220+CD11c+NK1.1+ cells identify them as a subset of NK cells. *J. Exp. Med.* 204: 2561–2568.
40. Chaudhry, U. I., G. Plitas, B. M. Burt, T. P. Kingham, J. R. Raab, and R. P. DeMatteo. 2007. NK dendritic cells expanded in IL-15 exhibit antitumor responses in vivo. *J. Immunol.* 179: 4654–4660.
41. Lin, M. L., Y. Zhan, S. L. Nutt, J. Brady, M. Wojtasiak, A. G. Brooks, and A. M. Lew. 2006. NK cells promote peritoneal xenograft rejection through an IFN-gamma-dependent mechanism. *Xenotransplantation* 13: 536–546.
42. Cascalho, M., and J. L. Platt. 2001. The immunological barrier to xeno-transplantation. *Immunity* 14: 437–446.

Supplementary figure legends

Figure S1. $CD11c^+B220^+CD122^+$ cells do not produce IFNα.

$CD11c^+B220^+CD122^+$ cells or $CD11c^+B220^+CD122^-$ pDCs were isolated from the $CD11c^+B220^+$ fraction or $CD11c^-B220^-$ fraction of NOD-*scid* mouse spleen cells using the MoFlo cell sorter. These fractions were cultured in RPMI 1640 medium (Invitrogen) containing 10% FCS in 96-well flat-bottomed plates at 37°C in 5% CO_2. To induce IFNα, cells were stimulated with 1μM CpG ODN 2216 (Sigma-Aldrich) for 48 h. Culture supernatants were collected and IFNα was assayed using the Verikine Mouse IFNα ELISA Kit (PBL Interferon Sources, Piscataway NJ).

Figure S2. Cytotoxicity is reduced *via* inhibition of an NKG2D receptor on $CD11c^+B220^+CD122^+$ and NK cells.

Non-RI cytotoxic assay was performed using the Cellular DNA Fragmentation ELISA kit (Roche Diagnostics, Mannheim, Germany) according to the manufacture's instructions. Sorted $CD11c^+B220^+CD122^+$ or NK cells from the spleens of NOD-*scid* mice were stained with anti-mouse NKG2D and isotype control antibody (Biolegend), respectively, and co-cultured with BrdU-labeled Yac-1 cells at various ratios for 4 h. After co-culturing, the supernatant was removed and amount of BrdU-labeled fragmented DNA was measured by ELISA. The percentage of lysis was calculated as described in *Cytotoxicity measurements* in the Materials and Methods.

Supplementary Figure S1

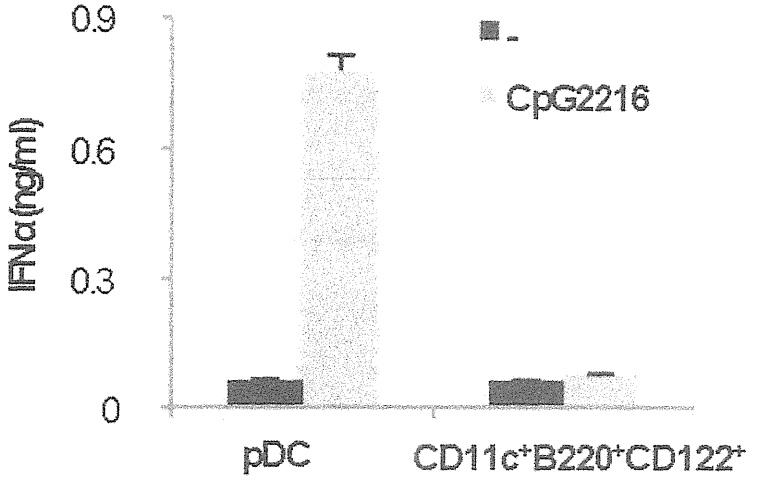

Supplementary Figure S2

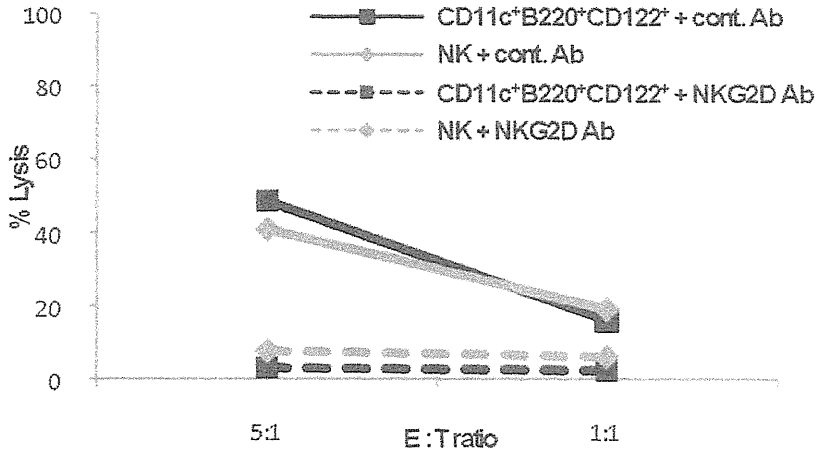

ELSEVIER

Experimental Hematology

Experimental Hematology 2012;40:953–963

Osteosclerosis and inhibition of human hematopoiesis in NOG mice expressing human Delta-like 1 in osteoblasts

Ryoji Ito[a,b], Naoko Negishi[c], Naoko Irie[d], Koichi Matsuo[d], Daisuke Suzuki[e], Ikumi Katano[a], Eri Hayakawa[a], Kenji Kawai[a], Tsutomu Kamisako[a], Tomoo Eto[a], Tomoyuki Ogura[a], Katsuto Hozumi[e], Kiyoshi Ando[f], Sadakazu Aiso[b], Norikazu Tamaoki[a], Sonoko Habu[c,e], and Mamoru Ito[a]

[a]*Central Institute for Experimental Animals, Kawasaki, Japan;* [b]*Department of Anatomy, Keio University School of Medicine, Tokyo, Japan;* [c]*Department of Immunology, Juntendo University School of Medicine, Tokyo, Japan;* [d]*Laboratory of Cell and Tissue Biology, Keio University School of Medicine, Tokyo, Japan;* [e]*Department of Immunology, Tokai University School of Medicine, Kanagawa, Japan;* [f]*Division of Hematopoiesis, Research Center for Regenerative Medicine and Department of Hematology, Tokai University School of Medicine, Kanagawa, Japan*

(Received 7 December 2010; revised 31 May 2012; accepted 19 June 2012)

NOD/Shi-scid IL2rγnull (NOG) mice with severe immunodeficiency are excellent recipients to generate "humanized" mice by the transplantation of human CD34$^+$ hematopoietic stem cells (HSCs). In this study, we developed NOG mice carrying a human Delta-like1 (DLL1) gene, which is a ligand of the Notch receptor and is known to be important in HSC maintenance and self-renewal. We also analyzed the effect of DLL1 signaling on human hematopoiesis and HSC maintenance using humanized DLL1 transgenic NOG mice. To develop DLL1 transgenic NOG (NOG-D1-Tg) mice, a transgenic vector consisting of a human DLL1 complementary DNA fragment placed downstream of the α1(I) collagen (Col1a1) promoter for expression specifically in osteoblasts was constructed. Human CD34$^+$ HSCs were transplanted into NOG-D1-Tg mice, and differentiation of lymphoid or myeloid lineage cells from human HSCs and maintenance of HSCs in bone marrow were analyzed. Severe osteosclerosis accompanied by increased bone mass and a decreased number of bone marrow cells were observed in NOG-D1-Tg mice. After human HSC transplantation, development of human B lymphocytes, but not T lymphocytes, was significantly suppressed in both bone marrow and the periphery of NOG-D1-Tg mice. Contrary to the initial expectation, retention of human CD34$^+$ HSCs was inhibited in the bone marrow of NOG-D1-Tg mice. In conclusion, our data suggest that the development of human B lymphocytes and HSC maintenance in osteosclerotic bone may be suppressed by introducing DLL1. These unique humanized mice with sclerotic bone reconstituted by human HSCs are useful models of hematopoiesis in patients with osteosclerosis, such as osteopetrosis, and for investigation of osteogenesis via Notch signaling. © 2012 ISEH - Society for Hematology and Stem Cells. Published by Elsevier Inc.

Recently, the remarkably advanced development of "humanized" mice with human hematopoietic systems has enabled us to analyze the differentiation of human lymphocytes from hematopoietic stem cells (HSCs) in vivo. We previously generated severe immunodeficient NOD/Shi-*scid* IL2rγ^{null} (NOG) mice, which were established by the introduction of the targeted IL-2rγ gene of IL-2rγ knockout mice [1] into NOD/Shi-*scid* mice [2,3] by backcross mating. They showed an extremely high engraftment rate of transplanted human HSCs compared with other immunodeficient mice due to their higher immunodeficiency, which is the lack of T, B, and natural killer cells and reduced functions of macrophage and dendritic cells. Furthermore, mature human T cells differentiated from cord blood CD34$^+$ HSCs could be detected in NOG mouse peripheries. Therefore, NOG mice are considered excellent models of humanized mice, where human immune cells are well developed and differentiated after transfer of human HSCs [3–5].

To evaluate human HSC development activity, xenotransplantation models using immunodeficient mice have been widely used as recipients. Yahata et al. identified CD34$^+$38$^-$ human long-term repopulating cells in cord blood, which are responsible for lifelong hematopoiesis in the bone marrow

Offprint requests to: Mamoru Ito, D.V.M., Ph.D., Central Institute for Experimental Animals, 3-25-12 Tonomachi, Kawasaki-ku, Kawasaki 210-0821, Japan; E-mail: mito@ciea.or.jp

Supplementary data related to this article can be found online at doi:10.1016/j.exphem.2012.07.002.

0301-472X/$ - see front matter.
http://dx.doi.org/10.1016/j.exphem.2012.07.002

microenvironment of NOG mice [6]. They also revealed that the quiescent human long-term repopulating cells localized to and interacted with the stem cell niche in NOG mice. Thus, humanized mice are available as the analysis tool for the features of human HSCs and interaction with their niches.

Notch receptors and their ligands are widely expressed in the process of hematopoiesis and play an essential role in T-cell lineage commitment [7–9]. Inactivation of Notch-1 leads to blockage of T-cell differentiation at an early stage with ectopic B-cell development in the thymus [7]. In contrast, transduction of an active form of Notch-1 induced ectopic T-cell development in the bone marrow (BM) with prevention of B-cell differentiation [8]. Furthermore, reconstitution of hematopoietic progenitor cells with overexpressing DLL1 or 4 led to T-cell development, even in the absence of the thymus [9]. DLL1 also acts on hematopoietic progenitor cells, resulting in induction of hematopoiesis, especially T-lineage cells, in in vitro studies in mice [10,11] and humans [12,13].

Several groups previously reported that osteoblasts in the trabecular bone are the major component of the HSC niche [14–18] and that Notch signaling is required for the maintenance of an undifferentiated state and for an increase in the number of HSCs in vivo [14,15]. Duncan et al. generated transgenic Notch reporter mice that expressed the enhanced green fluorescent protein (EGFP) reporter gene in cells that were actively signaling through Notch [15]. They demonstrated that lineage$^-$c-kit$^+$Sca1$^+$ (KSL) cells dramatically increased in EGFP$^+$ cells in a trabecular bone area. Moreover, EGFP$^+$ KSL cells have more potential for multilineage differentiation than do EGFP$^-$ KSL cells when using transgenic Notch receptor mice. These results suggest that Notch signaling greatly contributes to HSC maintenance and expansion in their niche.

Several groups succeeded in the expansion of human HSCs by Notch signaling in vitro [12,19–21]. Suzuki et al. used immobilized recombinant human DLL1-Fc chimeric protein in the presence of hematopoietic cytokines for expansion of human HSCs in vitro and performed an *scid*-repopulating cells assay to evaluate the cultured HSCs by transplanting them into NOG mice [21]. When cultured in a medium containing DLL1-Fc, chimerism of *scid*-repopulating cells increased by approximately sixfold in NOG mouse BM compared with the absence of DLL1-Fc. Additionally, these HSCs had a multidifferentiation potency into lymphoid and myeloid lineage cells in vivo. These findings indicated that the Notch signal induced by DLL1 resulted in the prompt expansion and maintenance of the undifferentiated state of human HSCs. However, little is understood about in vivo involvement of DLL1 in the HSC niche and Notch signaling in humans.

In this study, we first generated NOG mice carrying the human *DLL1* transgene (NOG-D1-Tg), in which the *DLL1* was specifically expressed in osteoblasts under the control of the Col1a1 promoter. We also investigated the capacity of human HSC retention and the development of human T or B lymphocytes and myeloid-lineage cells in the NOG-D1-Tg mice after human HSC transplantation.

Materials and methods

Generation of human NOG-D1-Tg mice

Nonobese diabetic (NOD/Shi) mice were purchased from CLEA Japan, Inc. (Tokyo, Japan), and NOD/Shi-*scid*-IL2rγ^{null} (NOG; formal name, NOD.Cg-*prkdc*^{scid}*il2rg*^{tm1Sug}/ShiJic) mice were maintained in the Central Institute for Experimental Animals under specific-pathogen-free conditions. Human *DLL1* complementary DNA (2.2 kb) was donated by Dr. T. Saito (Toray Industries, Inc., Kanagawa, Japan). A DNA fragment containing the 2.3-kb osteoblast-specific promoter region for the mouse *Col1a1* promoter [22] was provided by Dr. B. de Crombrugghe (University of Texas, Houston, TX, USA). The chicken β-globin 5′ HS4 insulator (2.4 kb) [23,24] was provided by Dr. G. M. Lefevre (National Institute of Health, Bethesda, MD, USA). These DNA fragments of the *Col1a1* promoter, insulator, and human *DLL1* were inserted into the pCMVb vector (Clontech, Inc., Mountain View, CA, USA) (Fig. 1A). To generate transgenic mice, the vector was digested by the *SfiI* restriction enzyme, the linearized fragment was injected into NOD mouse embryos, and the offspring with transgenes were further backcross-mated to NOG mice to introduce the *scid* and IL-2 rγ^{null} genes. All animal experiments were approved by the Institutional Animal Care and Use Committee and were performed in accordance with Central Institute for Experimental Animals guidelines.

Bone analysis

For histological analysis, femurs and tibias from NOG-D1-Tg or non-Tg NOG mice were fixed with 4% paraformaldehyde (Wako, Osaka, Japan) overnight and decalcified with 20% EDTA/phosphate-buffered saline (PBS) solution for 4 days. The solution was then changed to 70% EtOH, and the decalcified bones were embedded in paraffin. Sections 3-μm thick were placed on aminosilane-coated glass slides (Matsunami Glass, Osaka, Japan) and stained with hematoxylin (Sakura Finetek Japan, Tokyo, Japan) and eosin (Muto Kagaku, Tokyo, Japan). For microcomputed tomography, femurs were fixed in 4% paraformaldehyde, followed in 70% EtOH, air-dried overnight, and scanned using a microcomputed tomography apparatus (GE Explore Locus SP Specimen Scanner; GE Healthcare, Fairfield, CT, USA). Bone and marrow volume were calculated using TRI/3D BON software (RATOC System Engineering Co, Ltd, Tokyo, Japan).

Human HSC transplantation

Commercially available human cord blood–derived CD34$^+$ cells (Cat. No. 2C-101A, Lonza, Switzerland) were used in this study. The frozen cells were incubated for melting in a water bath at 37°C and moved quickly into PBS containing 2% fetal bovine serum. After washing with PBS, the viability of CD34$^+$ HSC was examined by 2.5% trypan blue exclusion, and cells with $>80\%$ viability were used for transplantation. NOG-D1-Tg and non-Tg mice were irradiated with 2.5 Gy using an x-ray system (MBR-1505R, Hitachi Medical Corp., Tokyo, Japan) 1 day before 5×10^4 human HSCs intravenous transplantation via tail vein. Engraftment and differentiation of human cells in BM, spleen,

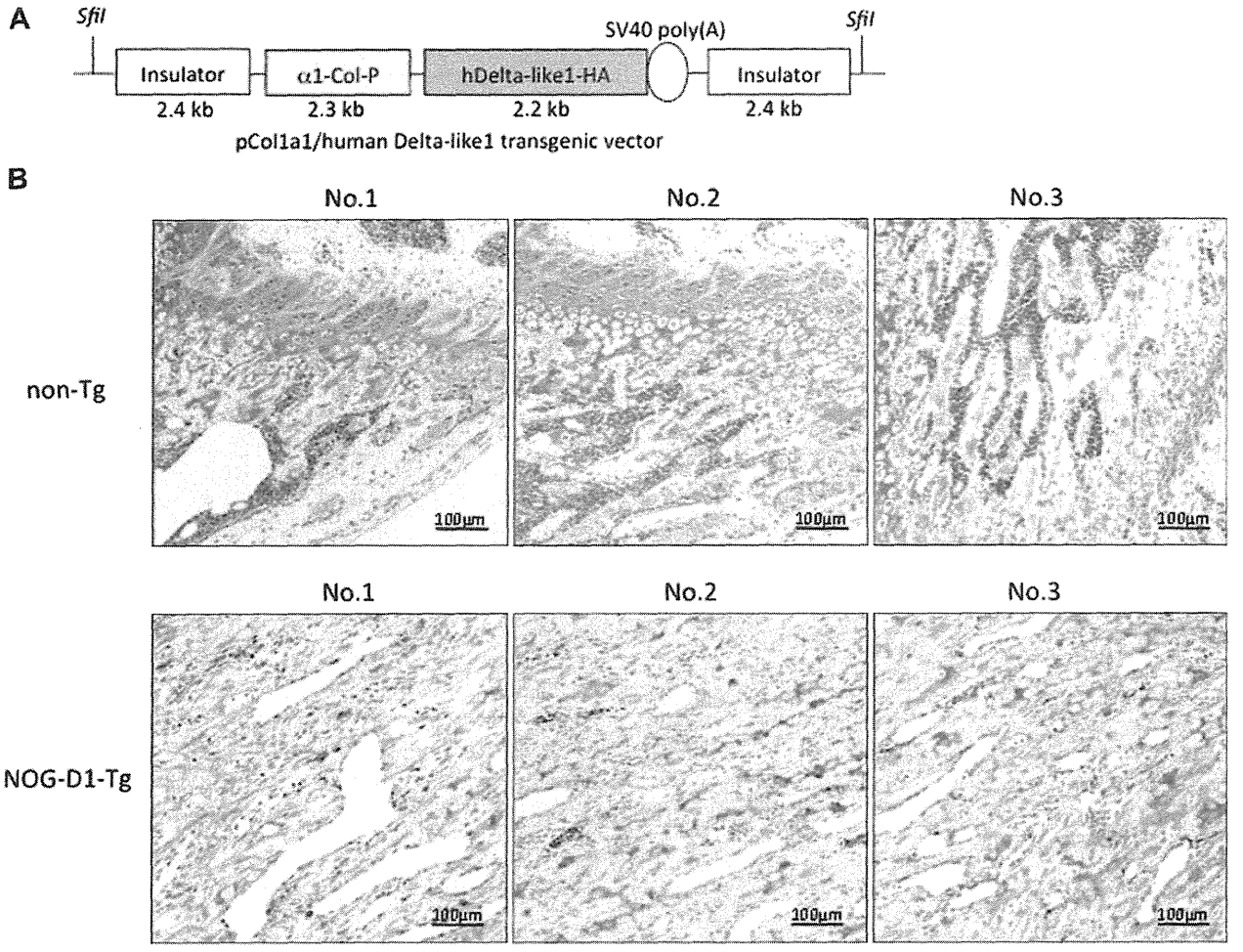

Figure 1. Generation of human Delta-like1 transgenic NOG mice. (A) A microinjected construct of human *DLL1* Tg vector fragments. (B) In immunohistochemistry, femurs from three NOG-D1-Tg mice and three non-Tg littermates were stained with an anti–hDelta-like-1 antibody. Human Delta like-1–positive cells are represented by brown coloration.

and peripheral blood (PB) were analyzed by flow cytometry staining with anti-human antibodies.

Flow cytometry

BM, PB, and spleens were obtained from the mice transplanted with human HSCs and prepared as single mononuclear cell suspensions using BD Pharm-Lyse (Becton Dickinson, BD Biosciences, San José, CA, USA) to remove red blood cells. Cells were incubated for 30 minutes at 4°C under protection from light with a mixture of appropriate fluorescently labeled monoclonal antibodies. After washing with 1% fetal bovine serum/PBS, cells were suspended in propidium iodide solution (BD Biosciences), followed by multicolor flow cytometry with FACS Canto (BD Biosciences), and analyzed by FACS Diva software (BD Biosciences). The engraftment ratio of human cells was expressed as the percentage of human $CD45^+$ cells out of total mononuclear cells (mice plus humans), excluding erythrocytes. The antibodies used for recognition of the cell surface molecules were anti-human CD45-allophycocyanin-Cy7 (BD Biosciences), CD33-fluorescein isothiocyanate (FITC; BD Biosciences), CD38-FITC (BD Biosciences), IgM-FITC (BioLegend, San Diego, CA, USA), lineage cocktail-FITC (BD Biosciences), CD19-phycoerythrin (PE) (Beckman Coulter, Inc., Brea, CA, USA), CD3-PE-Cy7 (Beckman Coulter), IgD-PE-Cy-7 (BioLegend), CD10-PE-Cy7 (BioLegend), and CD34-PE-Cy7 (BioLegend), CD20-allophycocyanin (BioLegend), anti-mouse c-kit–allophycocyanin (BioLegend), lineage cocktail-PE (BioLegend), and Sca-1-FITC (eBioscience, San Diego, CA, USA).

Immunohistochemistry

Sections were prepared in the same manner as described for the bone analysis. They were immunostained by the universal immunoenzyme polymer method (Nichirei, Tokyo, Japan). After deparaffinization, sections were incubated with an anti-human DLL1 antibody (Abcam, Inc., Tokyo, Japan) and an anti-hCD34 antibody (Dako Cytomation, Glostrup, Denmark) overnight at 4°C and then serially incubated with peroxidase-labeled polymer-conjugated anti-mouse or anti-rabbit antibody (Histofine Simplestain Max-PO; Nichirei) for 30 minutes at room temperature. For color development, these sections were incubated with 0.02% 3,3′-diaminobenzidine

(Dojindo, Kumamoto, Japan) substrate solution containing 0.006% H_2O_2. Immunostained sections were counterstained with hematoxylin (Sakura Finetek, Japan) for visualization of nuclei.

Statistical analysis

Mean values and standard deviations were computed using Excel (Microsoft, Remond, WA, USA). Significant differences were calculated by Student's t test and shown as $*p < 0.05$ and $**p < 0.005$. A p value of <0.05 was considered statistically significant.

Results

Generation of NOG-D1-Tg mice

After microinjection the complementary DNA encoding human *DLL1* into NOD mouse embryos, we obtained 9 Tg founders (#9, #12, #39, #40, #56, #58, #67, #71, and #78) and confirmed the expression of the *DLL1* transgene in femurs in two lines (#58 and #78). We decided to use #58 as human *DLL1* transgenic NOG mice (NOG-D1-Tg) in this study because the DLL1 protein level was higher than that in #78 (data not shown).

The expression of the human *DLL1* transgene in femoral bones of NOG-D1-Tg mice was evaluated by immunohistochemistry using an anti-human DLL1 antibody. The human DLL1 protein was expressed in a small marrow space in femurs from three 8-week-old NOG-D1-Tg mice, but not from three littermate non-Tg mice, as shown by intense brown coloration (Fig. 1B).

Severe osteosclerosis in NOG-D1-Tg mice

We further investigated the characteristics of the BM of NOG-D1-Tg mice. As shown in Figure 2A, almost all marrow areas in the proximal tibias from 2-week-old and 8-week-old NOG-D1-Tg mice were filled with bone mass stained with eosin. This increase in bone mass was observed in both sexes (data not shown). In the microcomputed tomography imaging, femurs from NOG-D1-Tg mice were occupied by a calcified area, and analysis on the whole femurs revealed an approximately 1.8-fold increase in total volume and 2.5-fold increase in bone volume. In contrast, marrow volume and marrow/total ratio were significantly decreased in NOG-D1-Tg mice (Fig. 2B). Thus, NOG-D1-Tg mice showed severe osteosclerosis and narrowing marrow spaces since juvenile ages. We compared the mouse mononuclear cell number and early HSC ratio defined by KSL cells in femurs from NOG-D1-Tg and non-Tg mice. As shown in Figure 2C, a 1.8-fold decrease in the mononuclear cell number was observed in NOG-D1-Tg mice. Although the absolute KSL cell number was also decreased in NOG-D1-Tg mice, the KSL cell ratio was similar between NOG-D1-Tg and non-Tg mice. These results suggest that the Notch signaling from DLL1 affects mouse osteoblasts, resulting in enhanced osteogenesis, but does not have an effect on mouse HSC self-renewal and maintenance.

Development of human lymphoid and myeloid cells

To investigate the effect of Notch signaling on human HSC development in humanized NOG-D1-Tg mice, we performed HSC transplantation and analyzed human lymphoid and myeloid-lineage cell differentiation. Figure 3A shows the scheme of human HSC transplantation and leukocyte analysis in NOG-D1-Tg or non-Tg mice. After transplantation of 5×10^4 human HSCs into 2.5-Gy-irradiated mice, we determined the cell number and ratio of engrafted human lymphoid and myeloid lineage cells in BM, spleen, and PB. As shown in Figure 3B, the number of total cells containing human and mouse cells was dramatically reduced in the BM of NOG-D1-Tg mice at 12 and 18 weeks after HSC transplantation. The engrafted cell number of human $CD45^+$ leukocytes was also reduced in BM, but not in spleen (Fig. 3C). The reduced leukocytes were almost $CD19^+$ B cells, and their development was significantly inhibited at 12 and 18 weeks. The numbers of $CD3^+$ T cells in BM and $CD33^+$ myeloid cells in the BM and spleen of NOG-D1-Tg mice also decreased at 18 weeks (Fig. 3C). The frequencies of $CD45^+$ leukocytes and $CD19^+$ B cells decreased slightly in the BM and spleen of NOG-D1-Tg mice, while the frequency of $CD3^+$ T cells increased in the spleen of these mice. No difference was observed in the frequency of $CD33^+$ myeloid cells (Fig. 3D). In PB, the frequency of human $CD45^+$ leukocytes in all non-Tg mice gradually increased from 4 to 16 weeks after human HSC transplantation, whereas it did not increase during this period in almost all NOG-D1-Tg mice, with the exception of one mouse (Fig. 3E). The frequency of $CD19^+$ B cells, in contrast to the frequency of $CD3^+$ T cells, in $CD45^+$ cells was also reduced in NOG-D1-Tg mice (Fig. 3F), which was also the case in the BM and spleen. While, human erythrocytes were not observed in the PB of either mouse strain after transfer of human HSCs (Supplementary Figure E1; online only, available at www.exphem.org). These findings indicate that the development of human B cells was remarkably inhibited in NOG-D1-Tg mice.

Human B-cell differentiation in NOG-D1-Tg mice

The number of human B cells was significantly reduced in NOD-D1-Tg mice as shown in Figure 3C, but it was unclear whether the process of B-cell differentiation was inhibited. We accordingly evaluated human $CD19^+$ cells using five surface molecules of human B cells in the BM and spleen of NOG-D1-Tg and non-Tg mice: CD34, CD10 (pro-B cell), IgM, IgD, and CD20 (mature B cell). In Figure 4A and B, the expression ratios of pro-B and mature B cell markers showed no differences in BM and spleen between NOG-D1-Tg and non-Tg mice. The averages of these subpopulations in B cells are shown in Figure 4C. In summary, B-cell differentiation was not affected in NOG-D1-Tg mice.

Human HSC maintenance in NOG-D1-Tg mice

To determine whether transplanted human HSCs were maintained in NOG-D1-Tg mice, we examined the

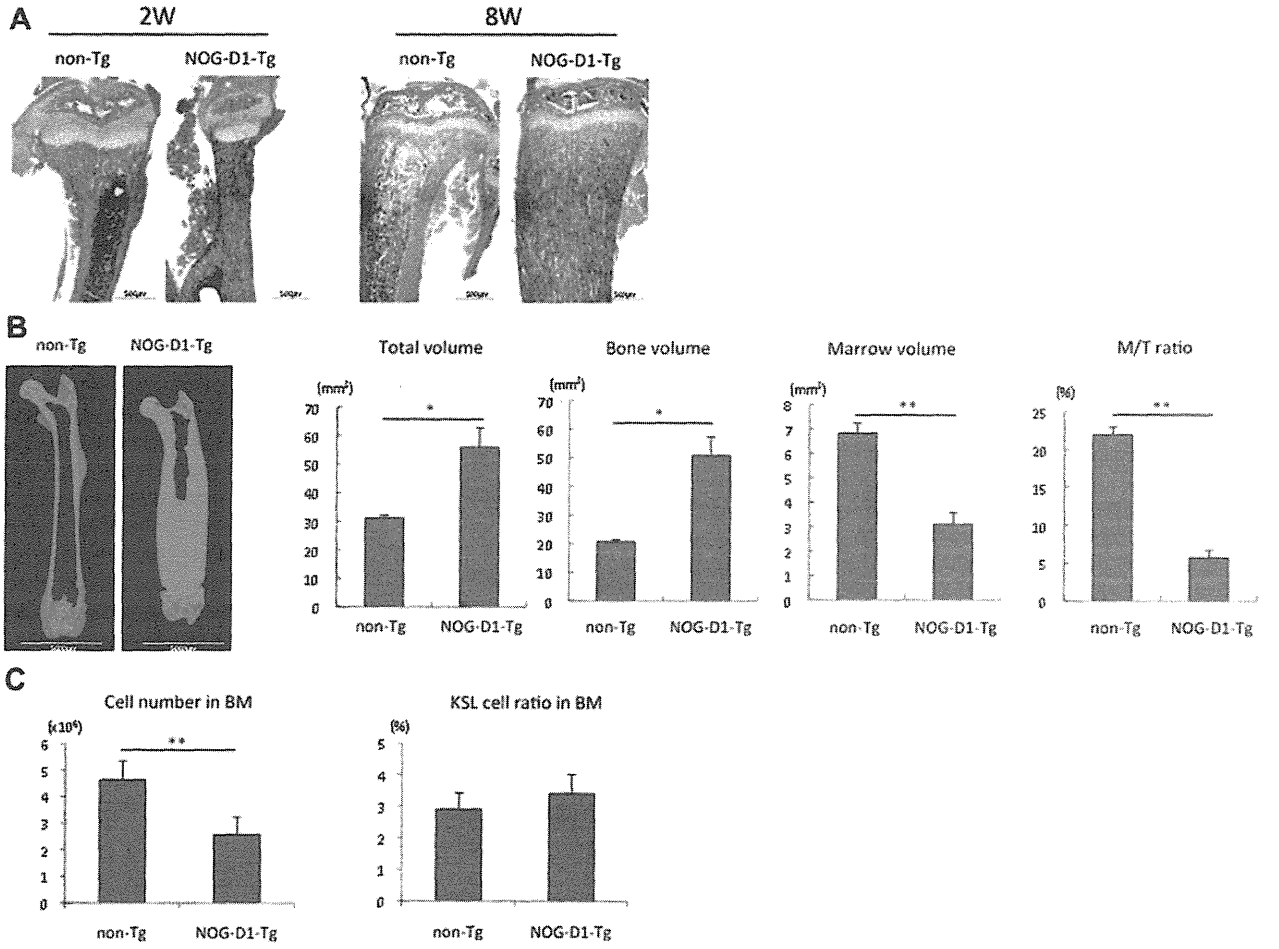

Figure 2. Severe osteosclerotic phenotype in NOG-D1-Tg mice. (**A**) Tibial bone sections in 2-week-old and 8-week-old NOG-D1-Tg mice and their non-Tg littermates were stained with hematoxylin and eosin. (**B**) The microcomputed tomography images of a femoral bone in 9-week-old NOG-D1-Tg and non-Tg mice. Bone and marrow spaces are shown in blue and red, respectively. Total volume (bone mass and marrow), bone volume, marrow volume, and marrow/total (M/T) ratio were calculated using TRI BON software (n = 3). (**C**) The total number of 8-week-old mouse mononuclear cells from femoral BM was counted under microscopy, and the ratio of lineage$^-$c-kit$^+$Sca1$^+$ (KSL) cells in CD45$^+$propidium iodide$^-$ cells was determined by flow cytometric analysis (n = 3). $*p < 0.05$ and $**p < 0.005$.

frequency and the number of HSCs in BM. First, we analyzed the frequency of lineage$^-$CD34$^+$ cells in the BM of NOG-D1-Tg mice. The sizes of these populations decreased at 6 and 18 weeks after HSC transplantation (Fig. 5A), while their frequencies decreased slightly at 18 weeks after HSC transplantation compared with those in the BM of non-Tg mice (Fig. 5B). We further examined the quantity of human HSCs in NOG-D1-Tg mice. The number of human HSCs (lineage$^-$CD34$^+$CD38$^-$) was drastically reduced (Fig. 5C), and the HSC ratio was decreased approximately fourfold in NOG-D1-Tg mice (Fig. 5D, E). When we investigated the localization of human HSCs in the femur by immunohistochemistry using an anti-human CD34 antibody, only a few human HSCs were observed in the femoral marrow space of NOG-D1-Tg mice compared with non-Tg mice (Fig. 5F). These results show that the microenvironment in the osteosclerotic bone of NOG-D1-Tg mice was not suitable for the maintenance of human HSCs.

Discussion

In this study, we developed novel transgenic NOG mice with the human Notch ligand *DLL1* gene, specifically expressed in osteoblasts under the control of the *Col1a1* promoter, to investigate human hematopoiesis under the influence of Notch signaling after transfer of human HSCs. Unexpected and severe osteosclerosis was observed in NOG-D1-Tg mice showing increased bone mass and narrow bone marrow spaces since juvenile age.

Han et al. previously reported cloning of complementary DNA encoding human *DLL1* [25]. They showed high conservation of amino acid sequences between human and mouse DLL proteins (89% in the extracellular domain,